CAMK
PAN

Comparison of spectral models for disc truncation in the hard state of GX 339-4

Marta Dziełak
A. Zdziarski, M. Szanecki, B. De Marco, A. Niedźwiecki and A. Markowitz

Nicolaus Copernicus Astronomical Center,
Polish Academy of Sciences
Warsaw, Poland

X-ray binary – GX 339-4

- accreting black hole

  min. $M=5.8M_{\odot}$ (Hynes et al. 2003)

- low mass companion

  fills Roche lobe

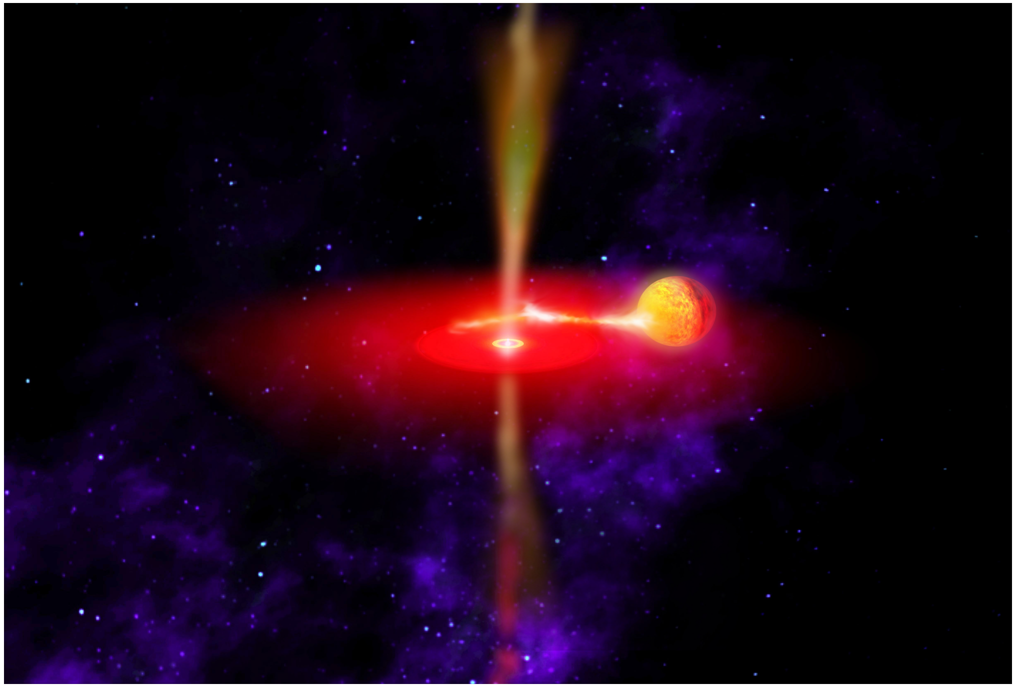

Flaring Black Hole (Artist's Concept)
Credit: NASA

Outburst of X-ray activity

Dziełak et al. 2019

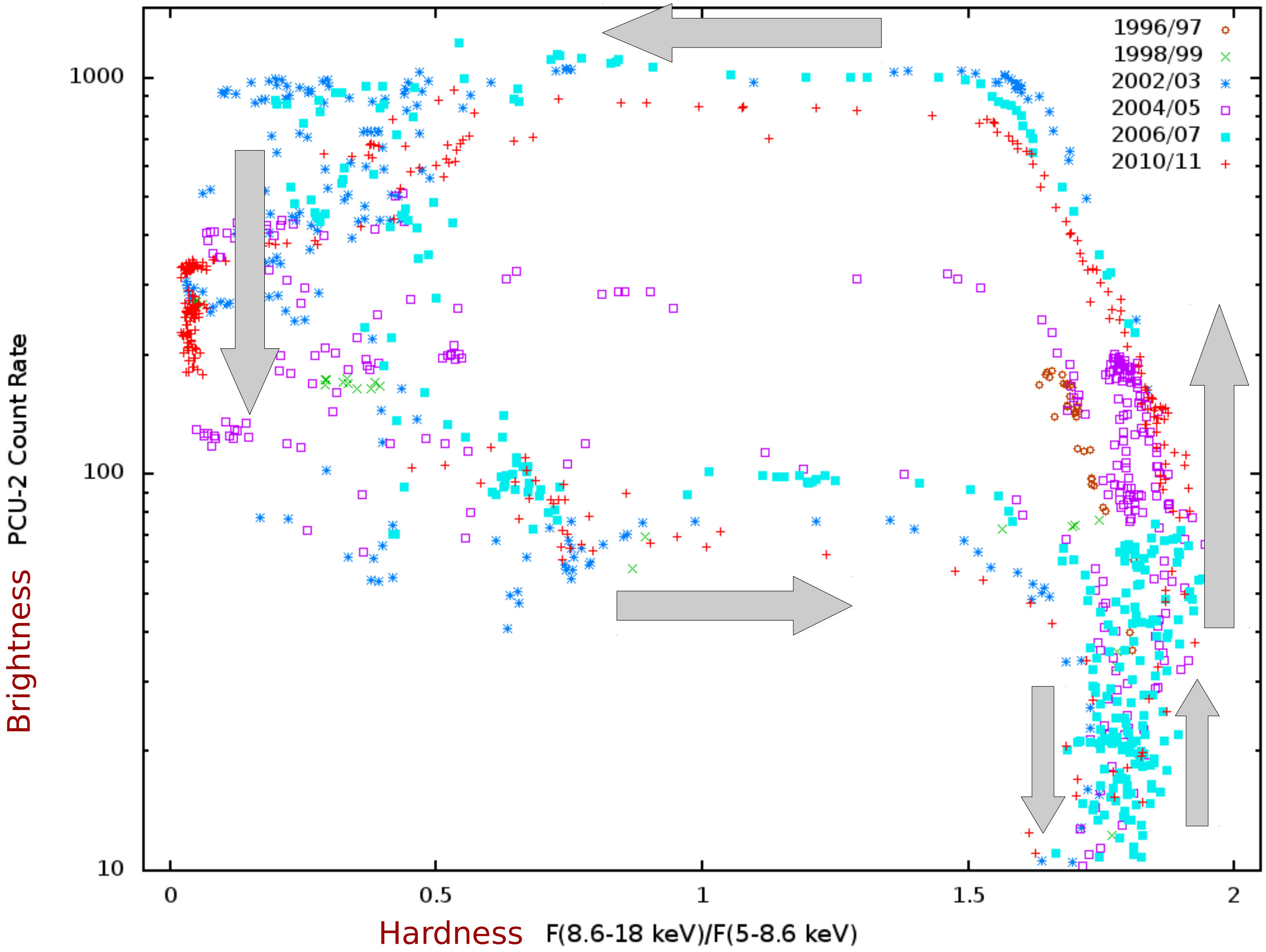

Outburst of X-ray activity

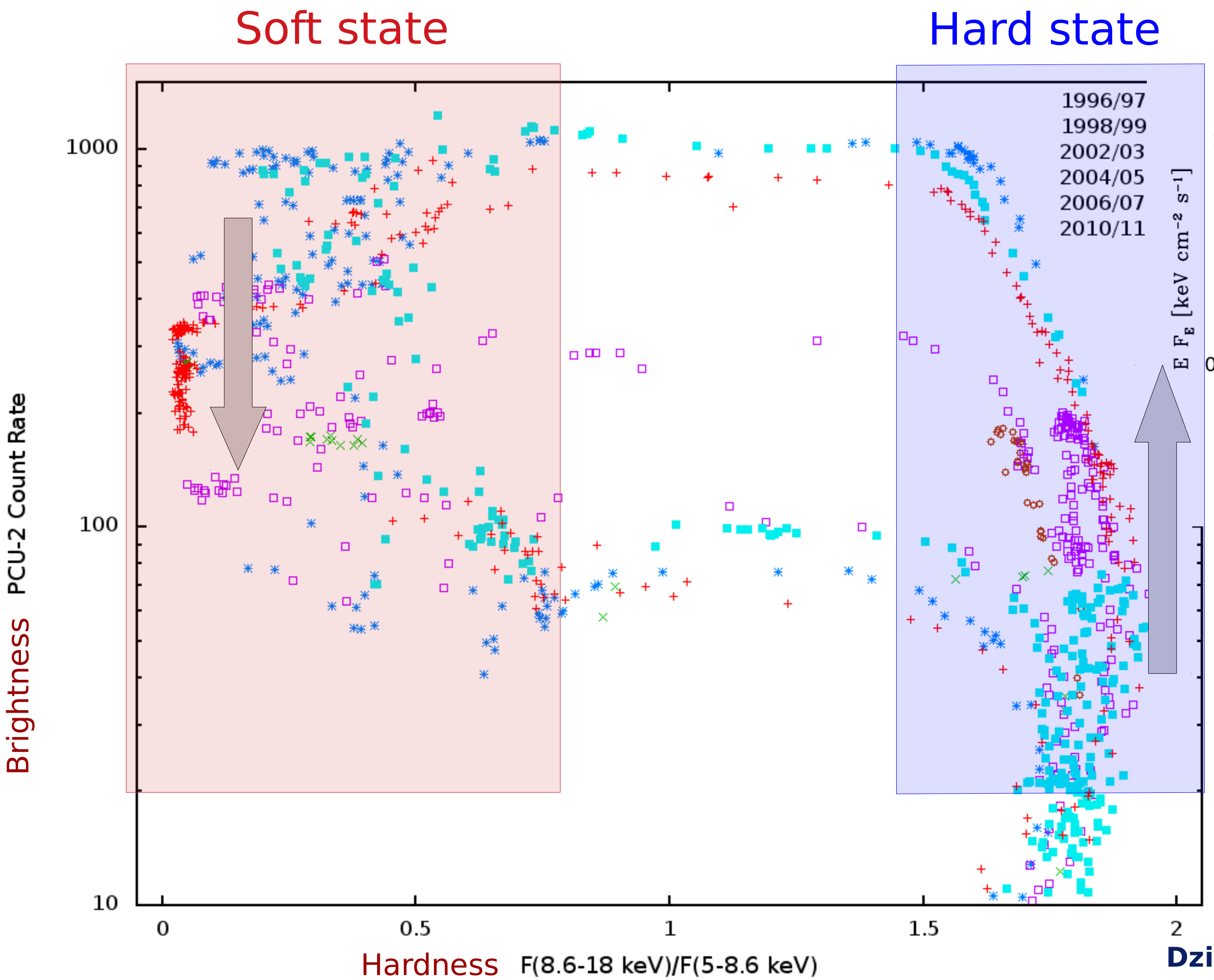

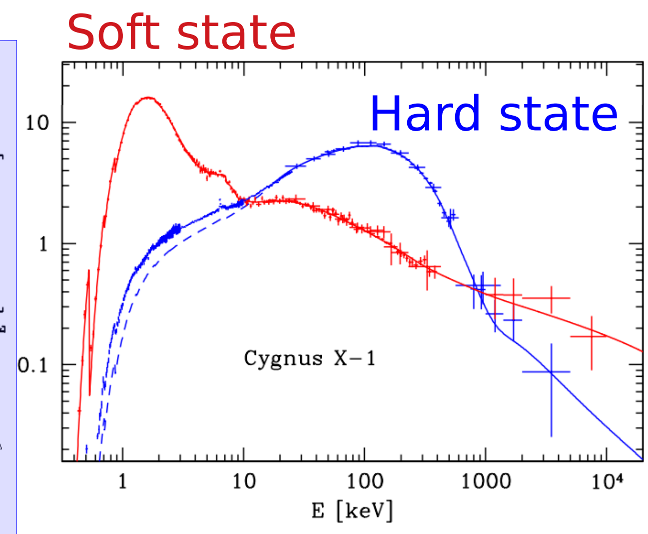

McConnell et al. 2002

Dziełak et al. 2019

Soft state

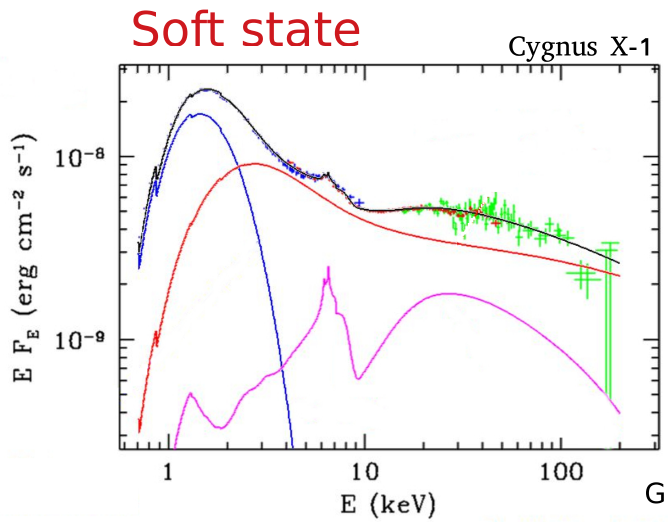

Gierliński et al. 1999

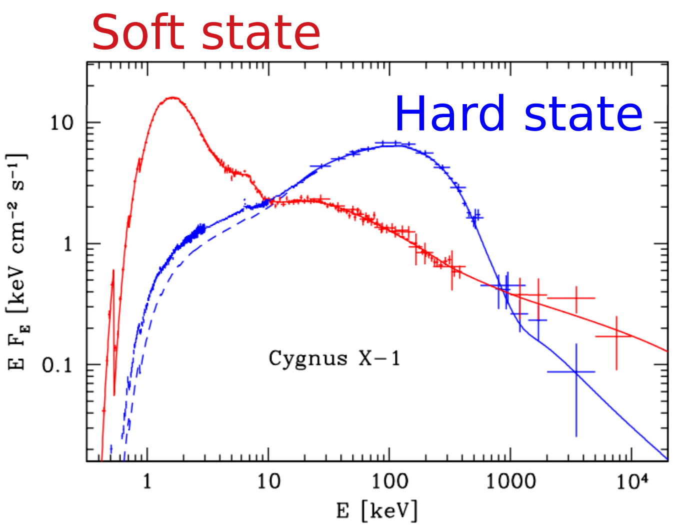

McConnell et al. 2002

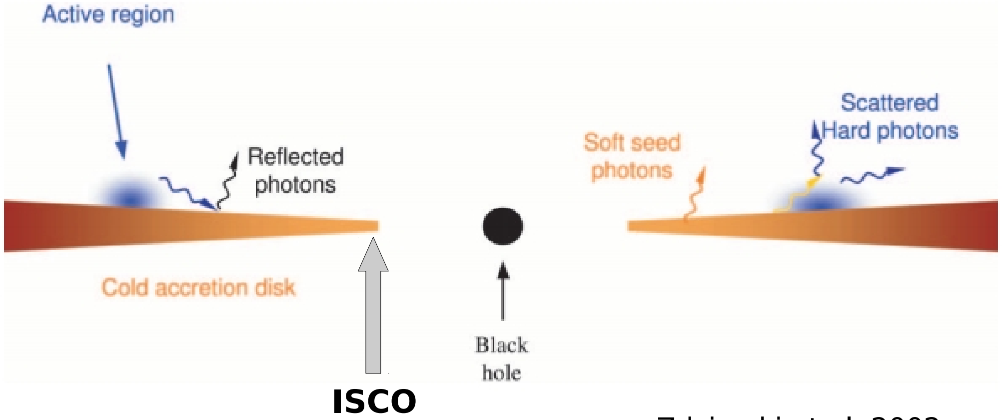

Zdziarski et al. 2002

Soft state

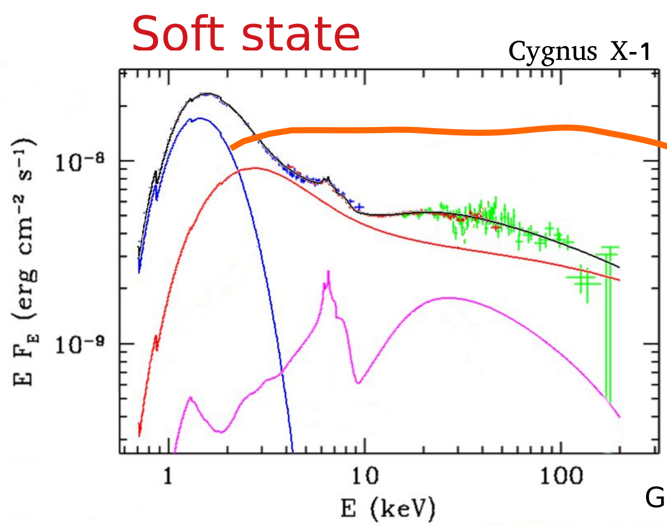

Gierliński et al. 1999

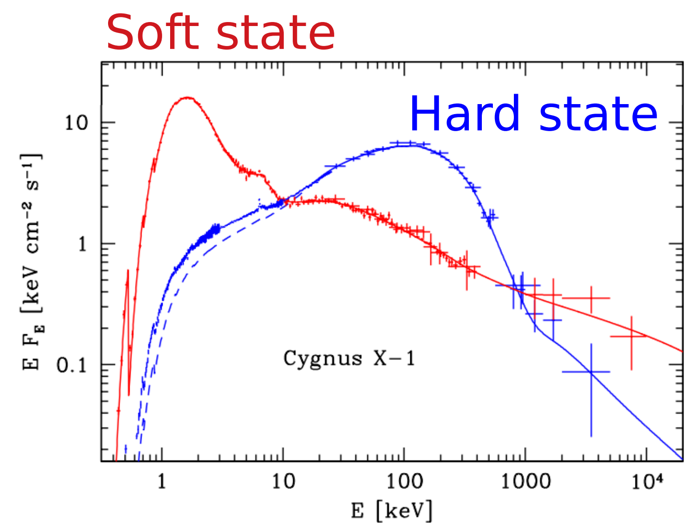

McConnell et al. 2002

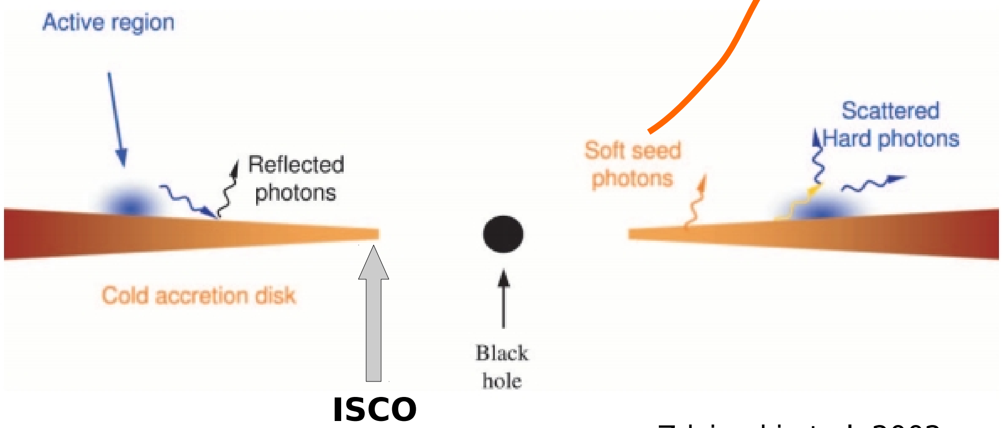

Zdziarski et al. 2002

Soft state

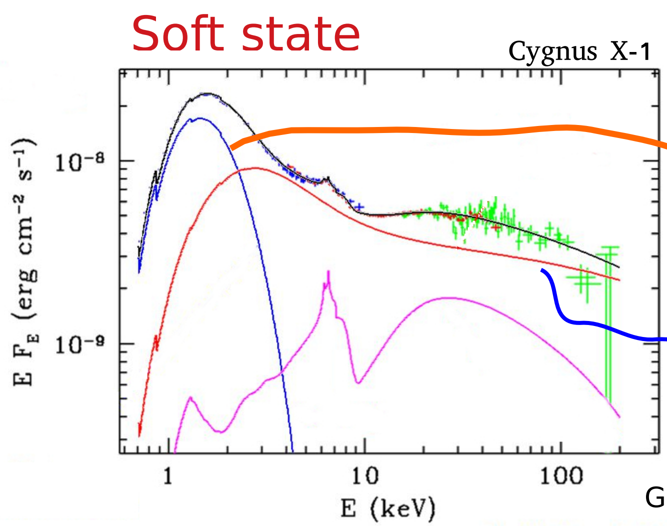

Gierliński et al. 1999

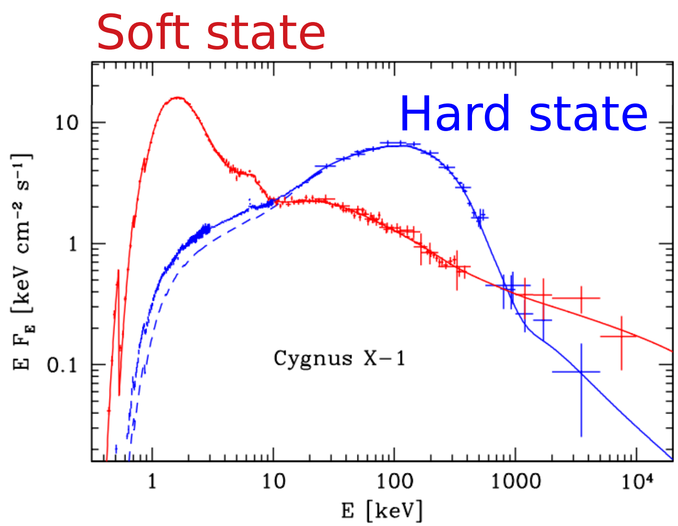

McConnell et al. 2002

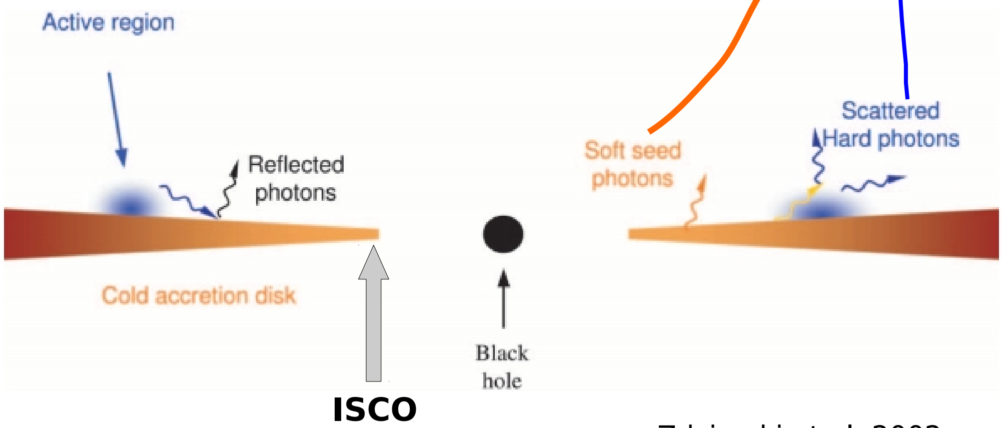

Zdziarski et al. 2002

Soft state

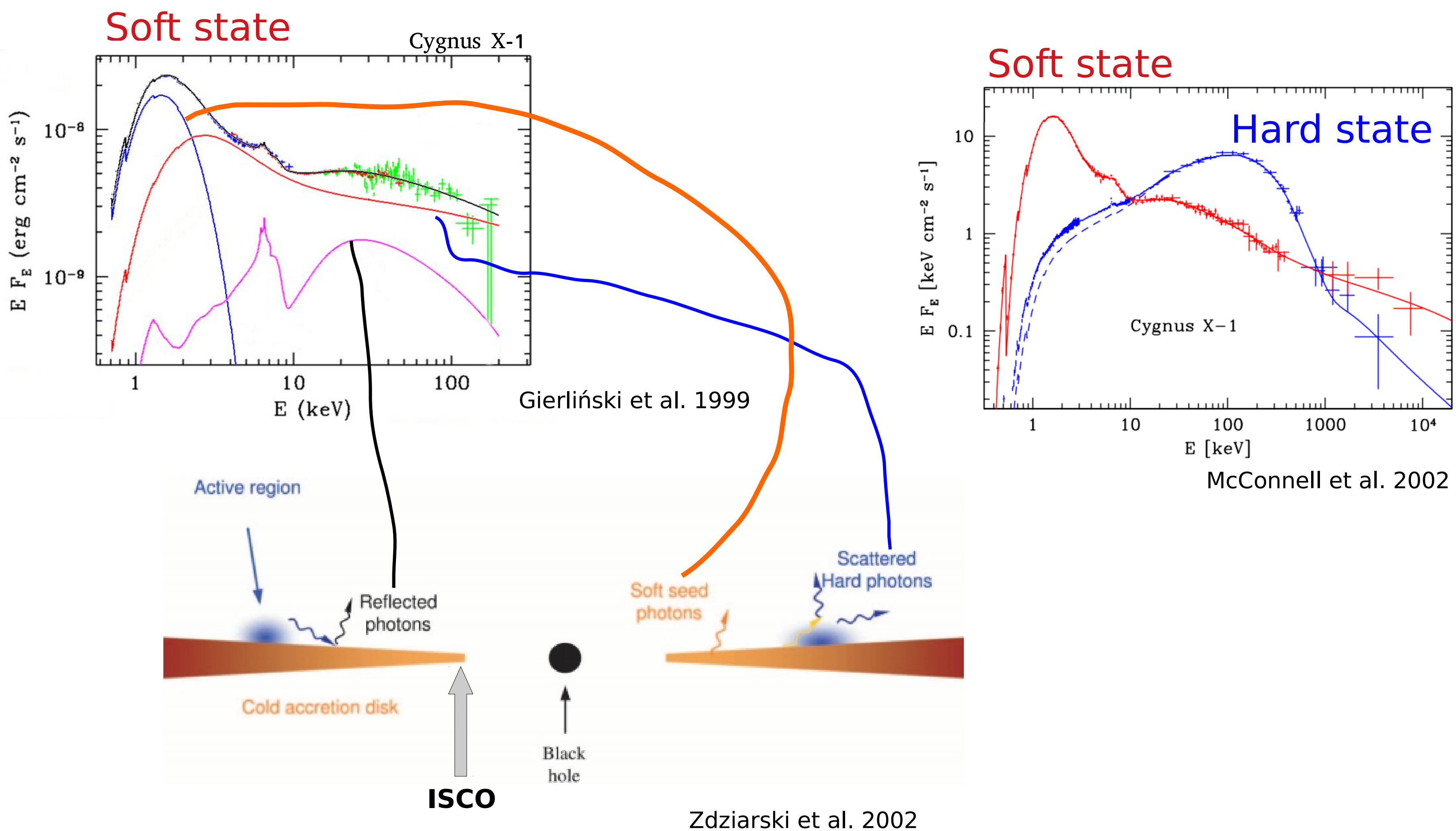
Soft state
Cygnus X-1
E F$_E$ (erg cm^{-2} s^{-1})
E (keV)
Gierliński et al. 1999
Soft state
Hard state
Cygnus X−1
E F$_E$ [keV cm^{-2} s^{-1}]
E [keV]
McConnell et al. 2002
Active region
Reflected photons
Soft seed photons
Scattered Hard photons
Cold accretion disk
Black hole
ISCO
Zdziarski et al. 2002

Outburst of X-ray activity

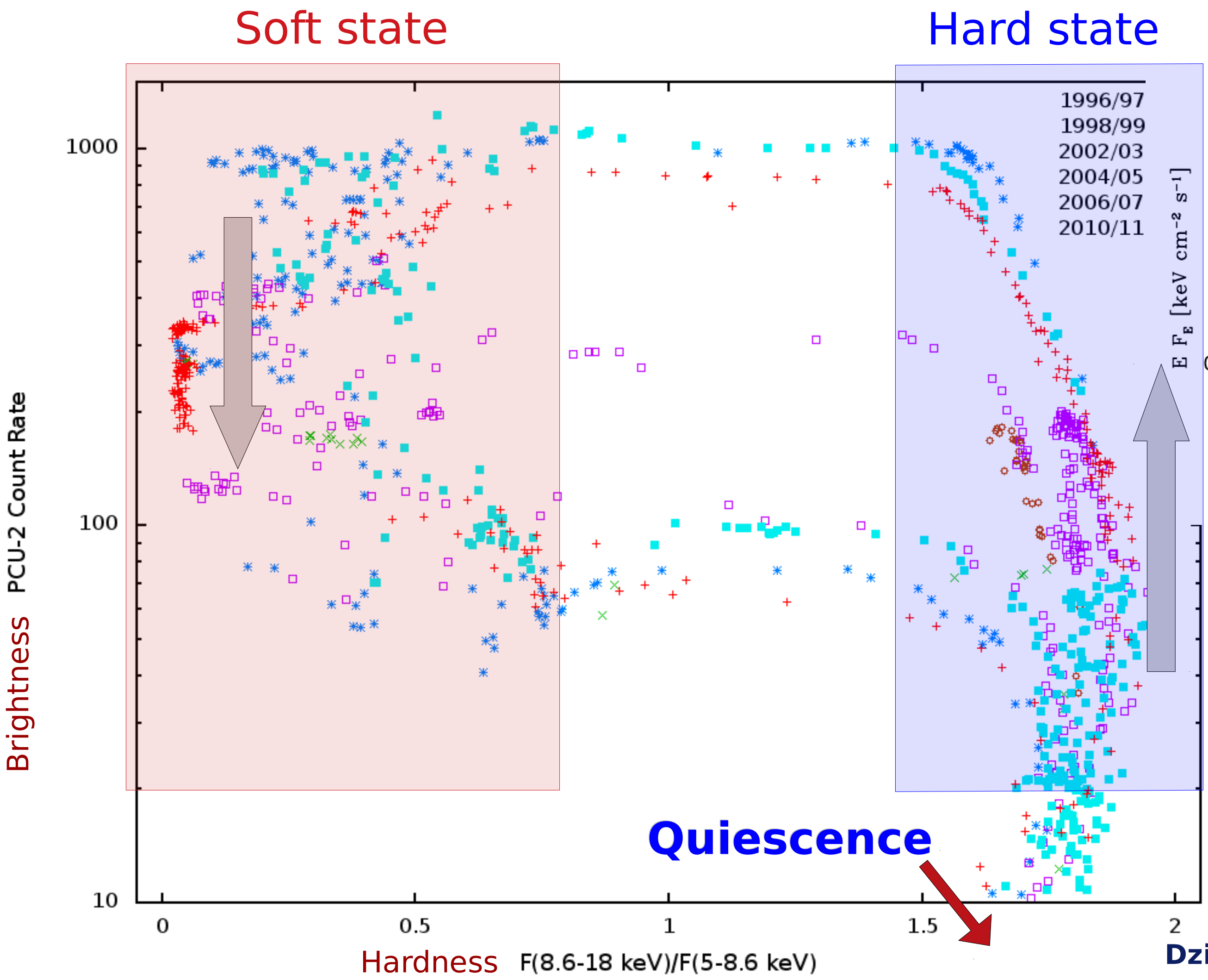

Dziełak et al. 2019

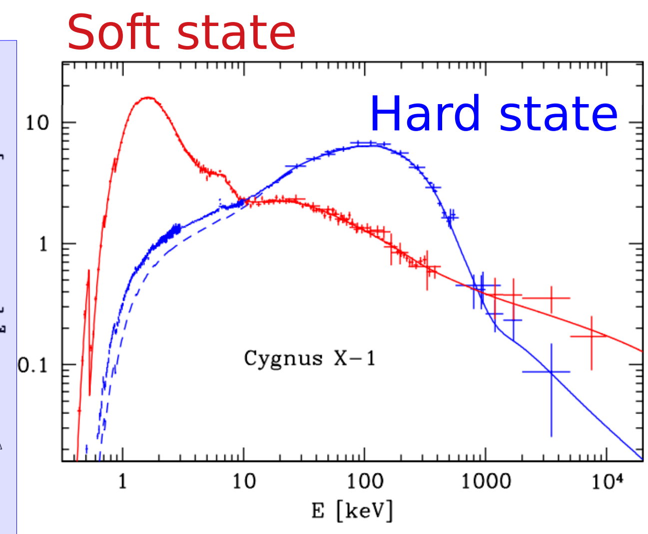

McConnell et al. 2002

Hard state

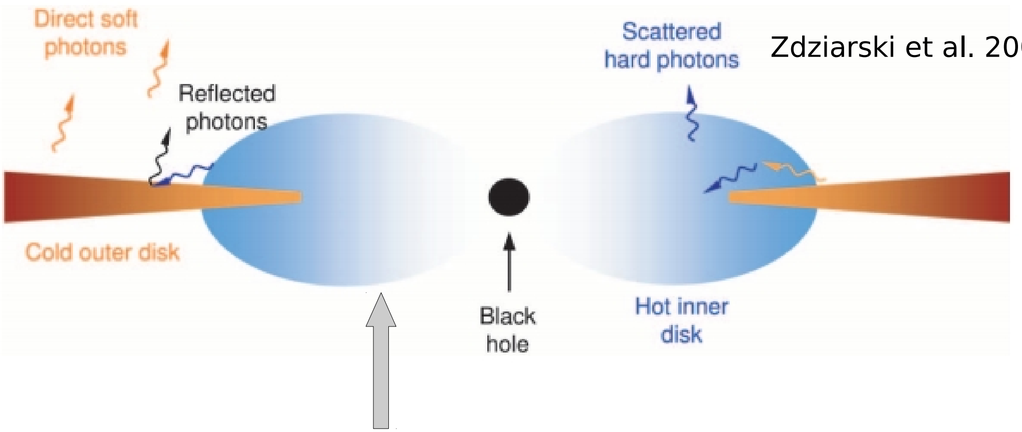

Zdziarski et al. 2002

ISCO

Soft state

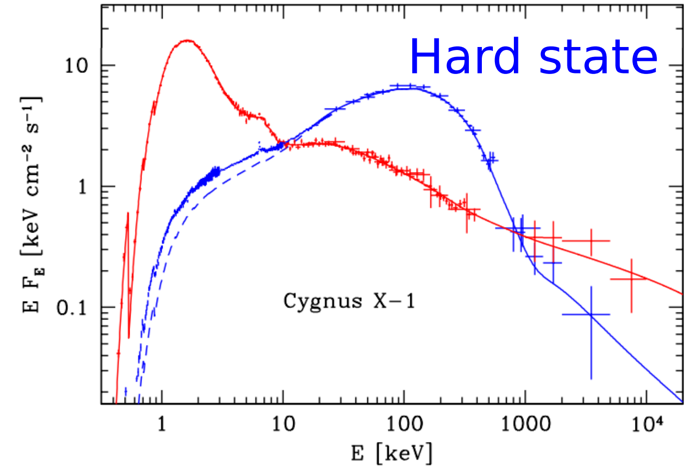

McConnell et al. 2002

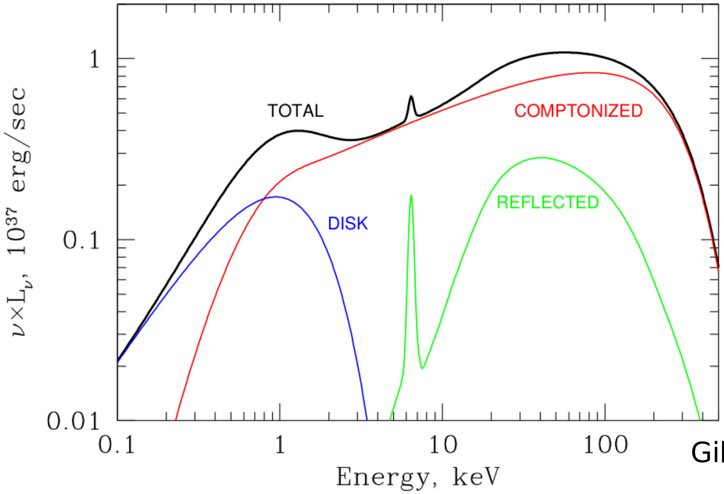

Gilfanov, 2009

Hard state

Hard state

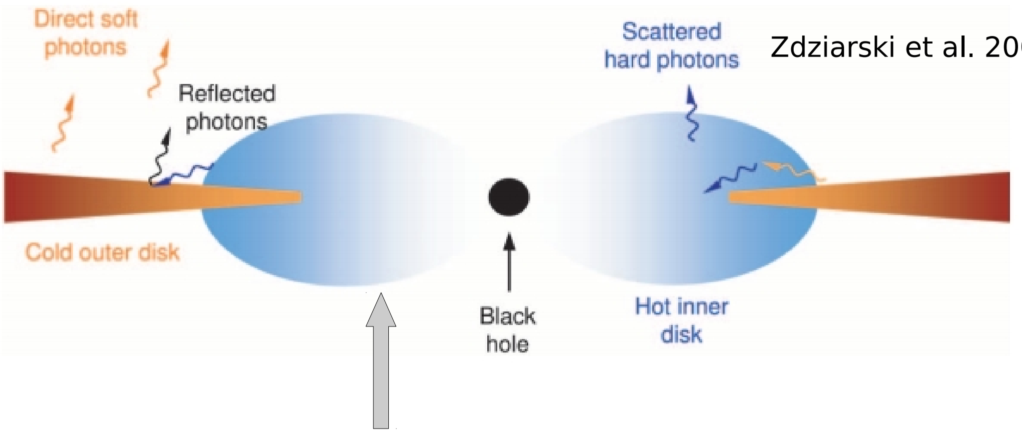

Zdziarski et al. 2002

Soft state

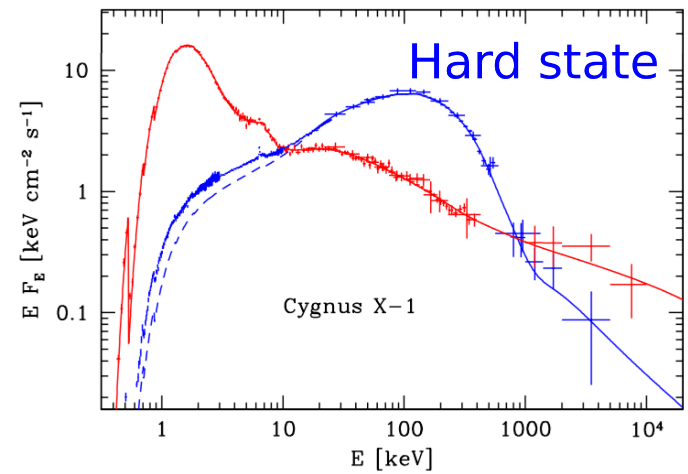

McConnell et al. 2002

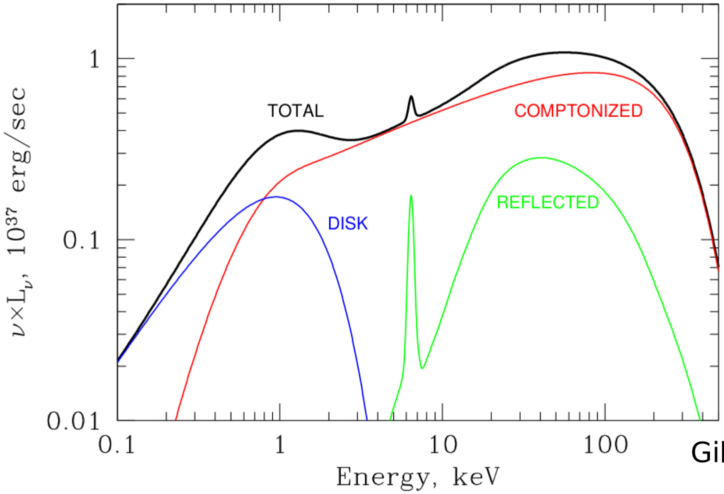

Gilfanov, 2009

Hard state

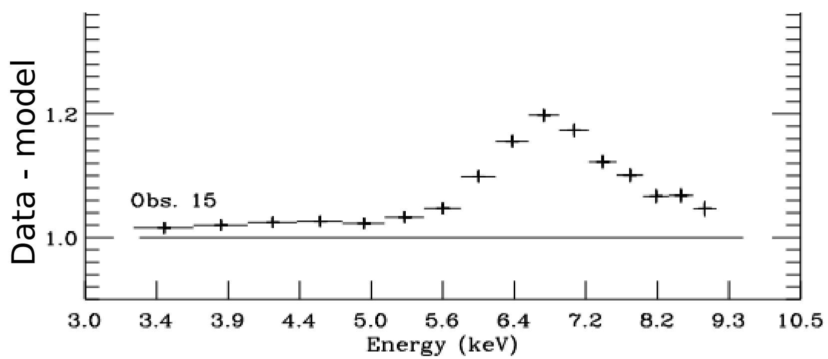

Broad Fe line in XTE J1748-228
Miller et al. 2001

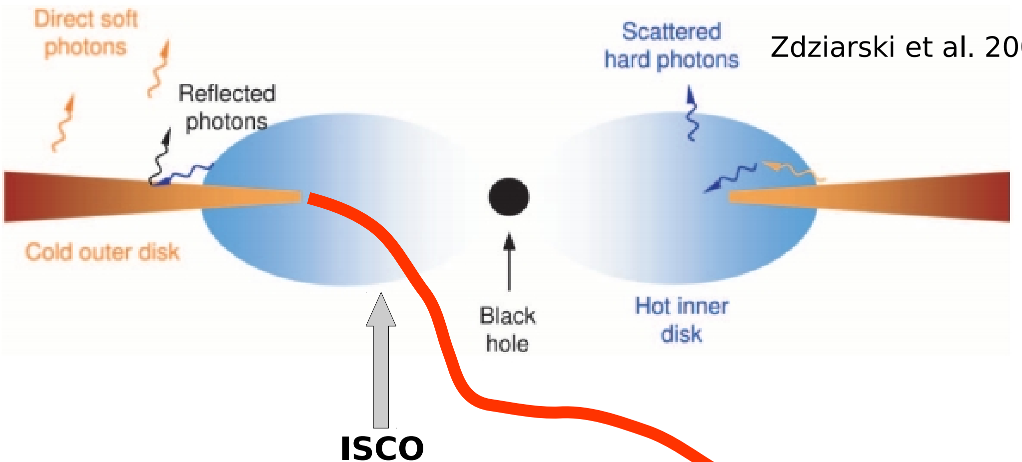

Zdziarski et al. 2002

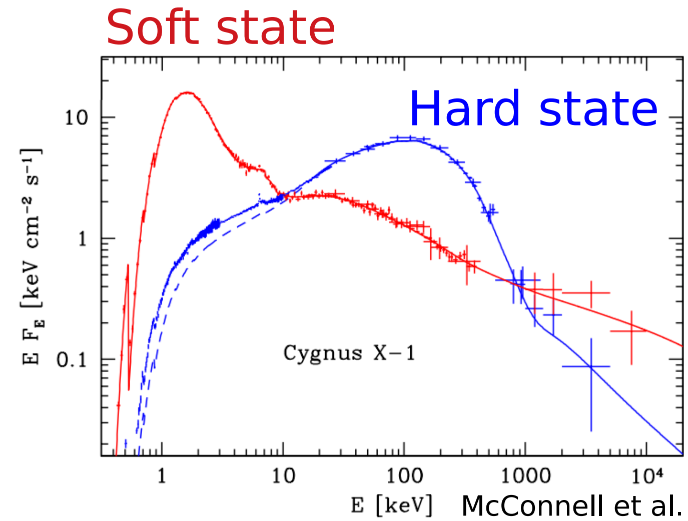

McConnell et al. 2002

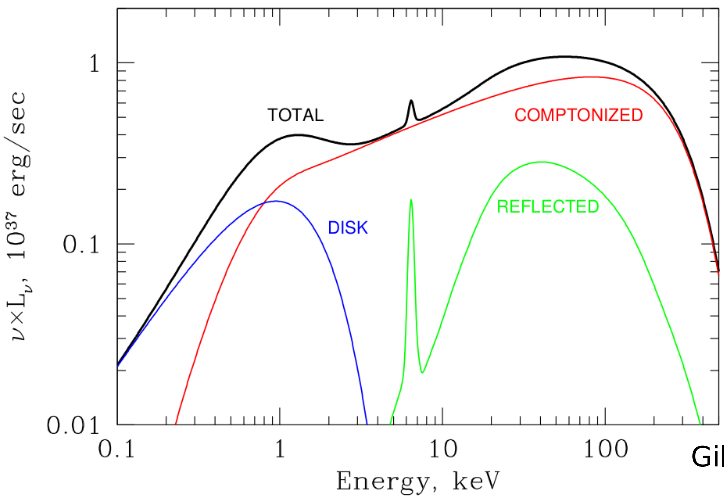

Gilfanov, 2009

Hard state

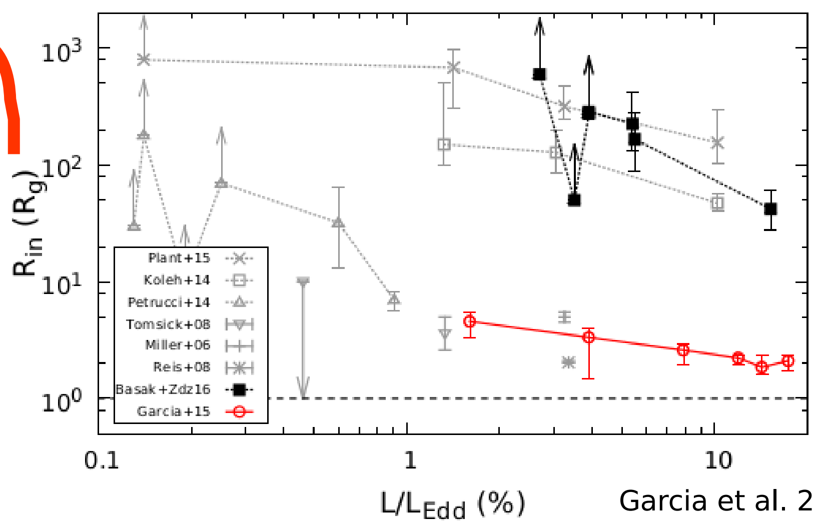

Garcia et al. 2015

Comparing spectral models

Dziełak et al. 2019

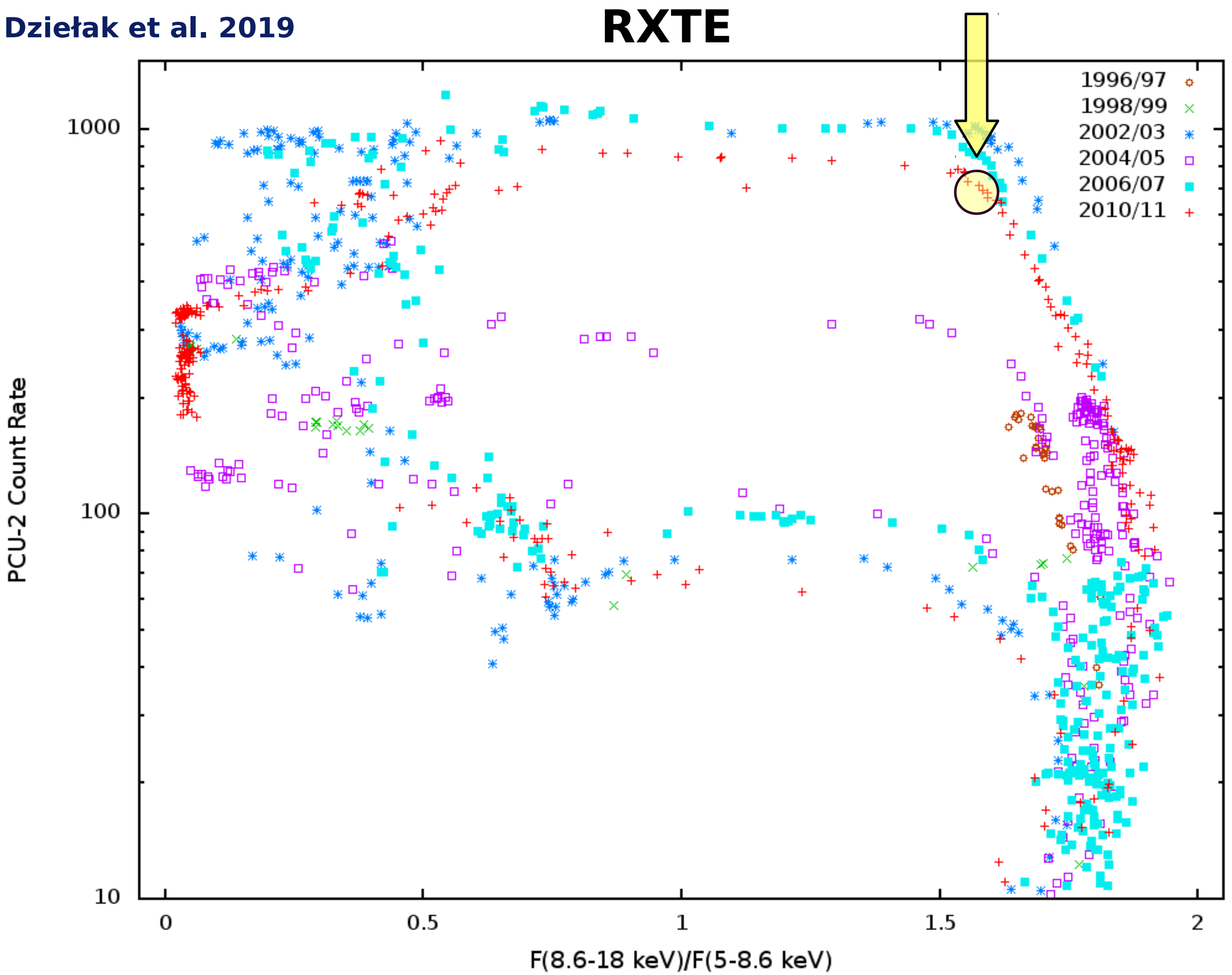

Comparing spectral models

Dziełak et al. 2019

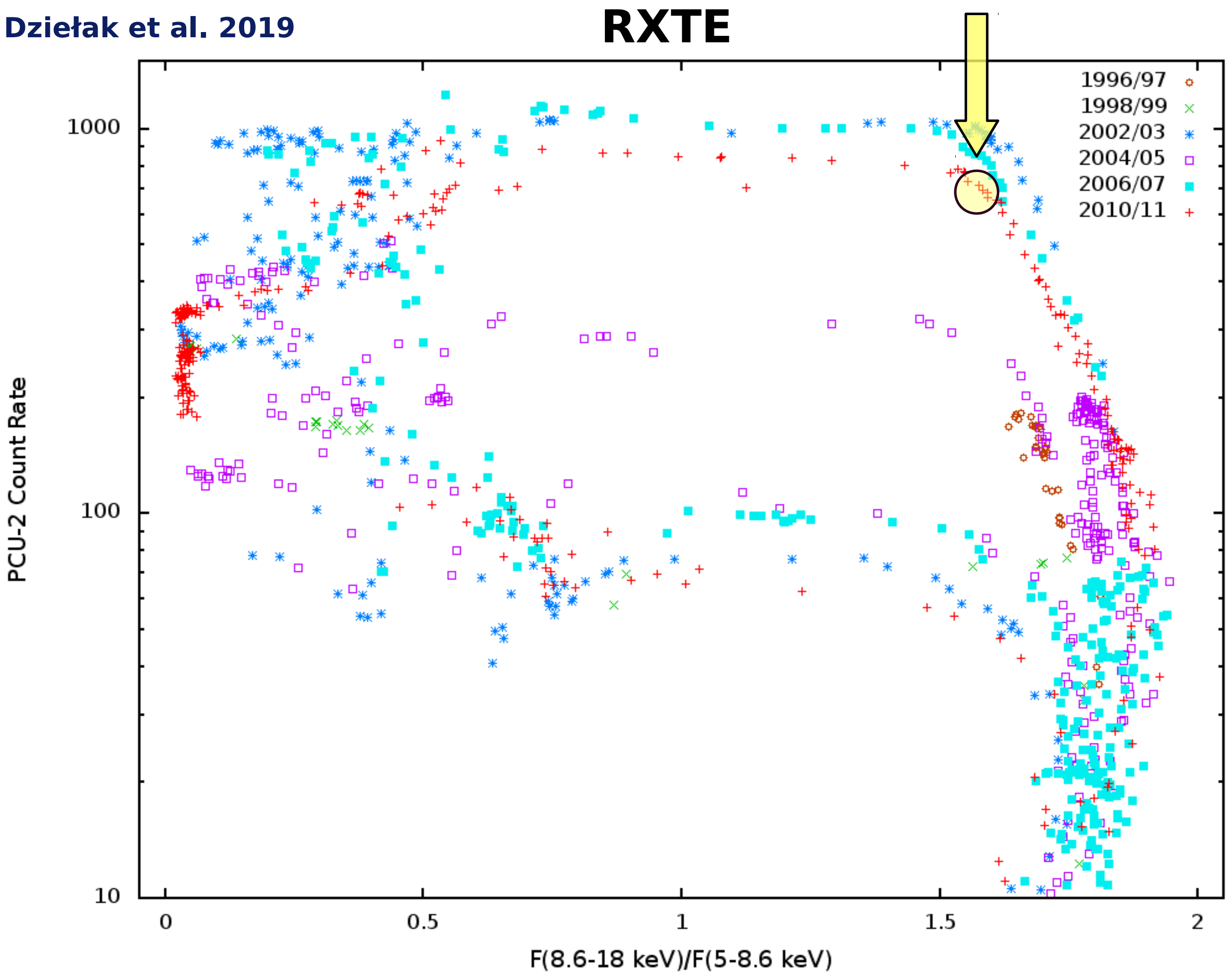

- averaged spectrum

Comparing spectral models

Dziełak et al. 2019

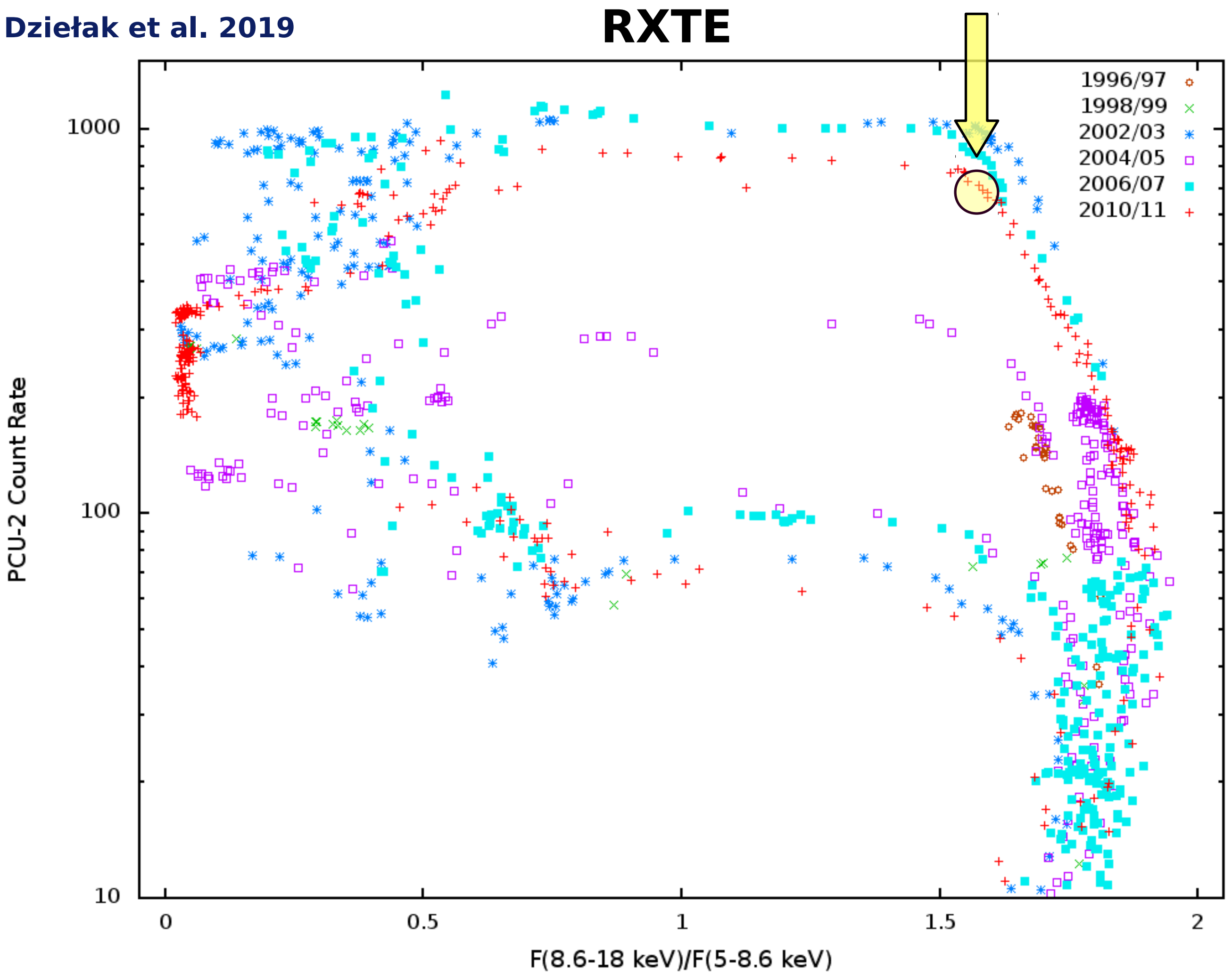

- averaged spectrum
- probed disc truncation:

Comparing spectral models

Dziełak et al. 2019

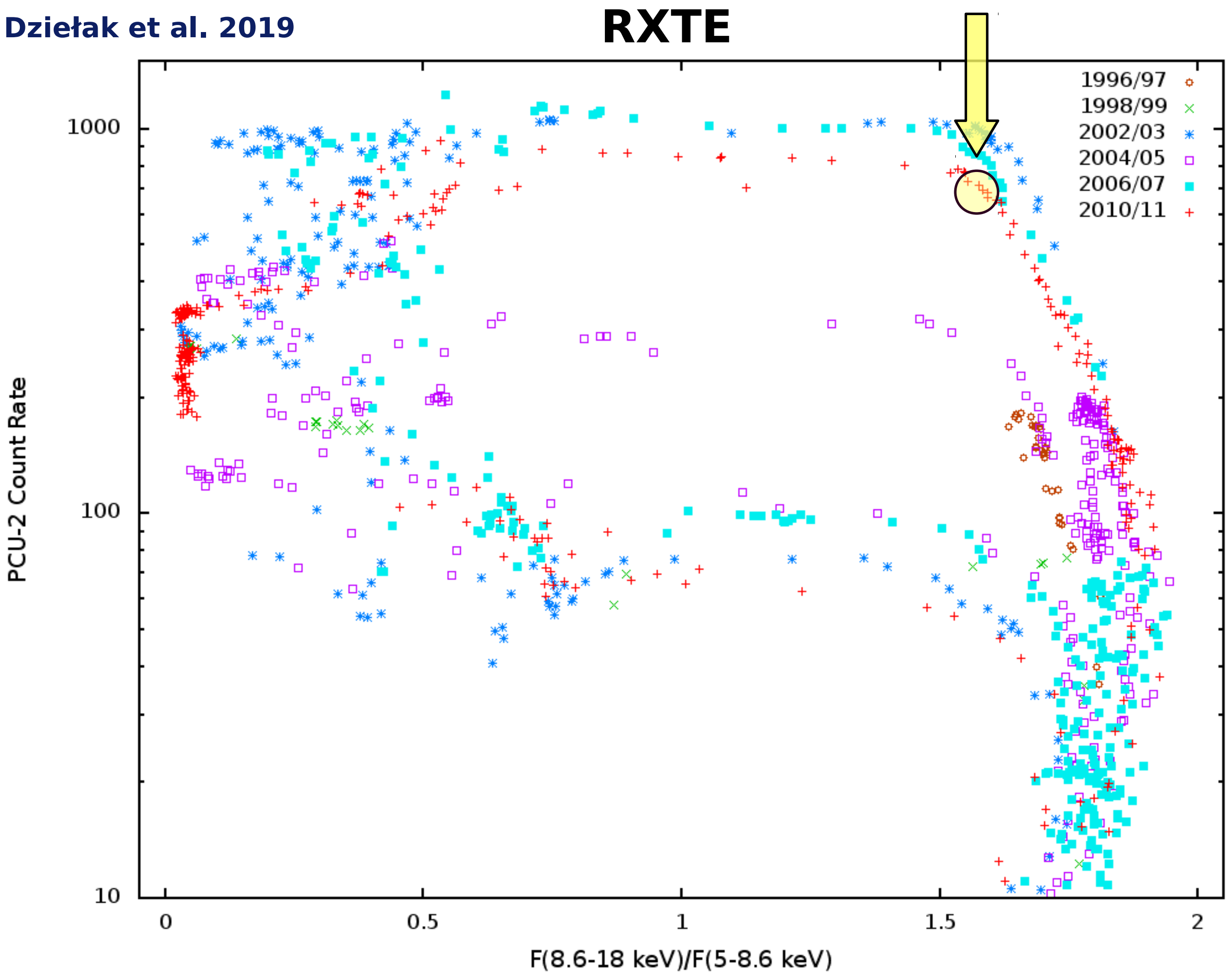

- averaged spectrum
- probed disc truncation:
    - reflection and relativistic broadening

Comparing spectral models

Dziełak et al. 2019

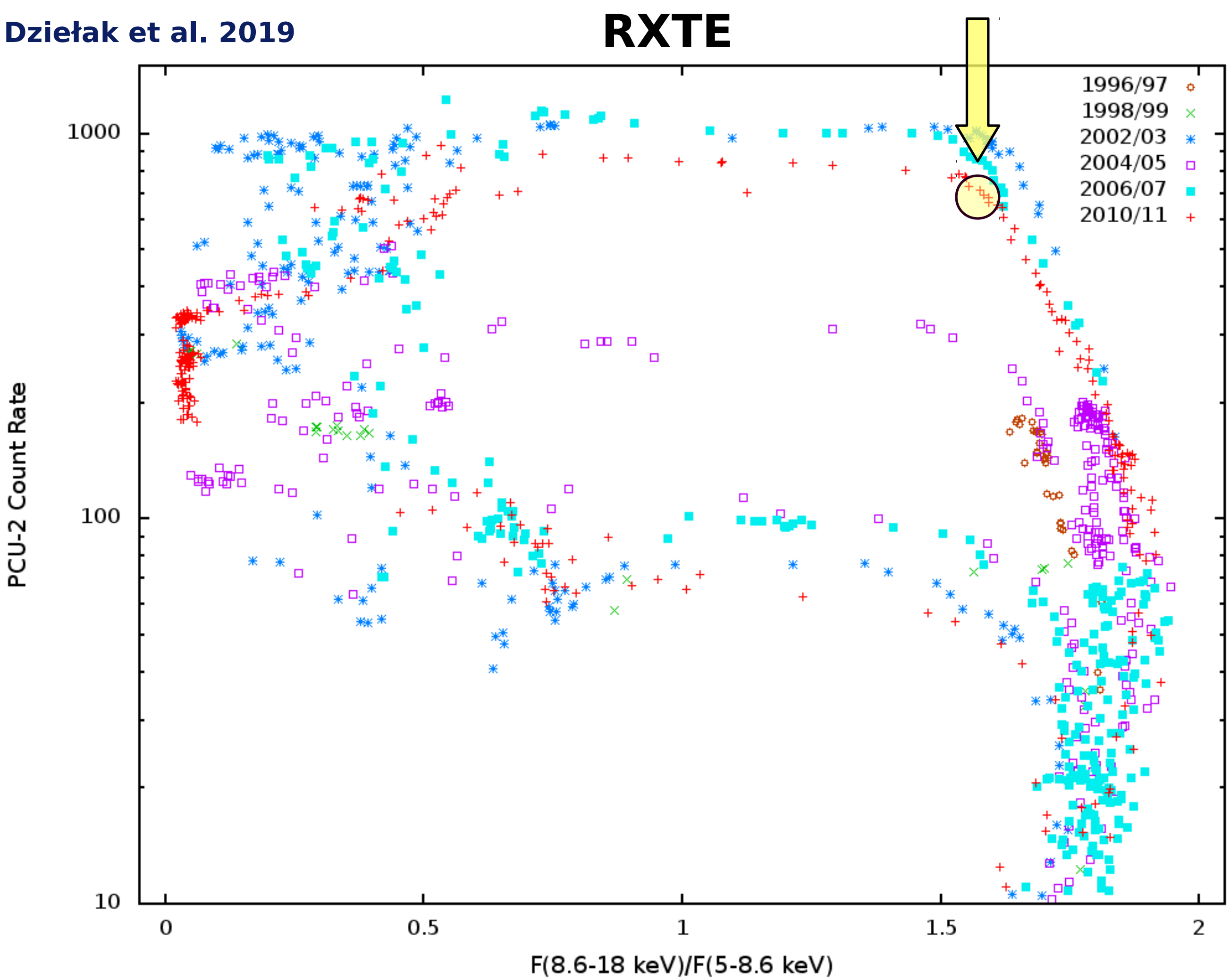

- averaged spectrum
- probed disc truncation:
  - reflection and relativistic broadening
  - two sets of codes:
    - relxill (Garcia, et al. 2014)
    - reflkerr[1] (Niedźwiecki, Szanecki, Zdziarski, 2019)

1) https://users.camk.edu.pl/mitsza/reflkerr/

Fitted models

reflkerr[1]:

- spectrum computed in **the local frame and redshifted**.

relxill:

- spectrum fitted in **the observer frame and blueshifted**.

1) https://users.camk.edu.pl/mitsza/reflkerr/

Fitted models

reflkerr[1]:

- spectrum computed in **the local frame and redshifted**.

→ photoionization

- the detailed calculations of **xillver at low energies**,

- the relativistically correct treatment of **ireflect at high energies** (Magdziarz & Zdziarski 1995).

1) https://users.camk.edu.pl/mitsza/reflkerr/

Fitted models

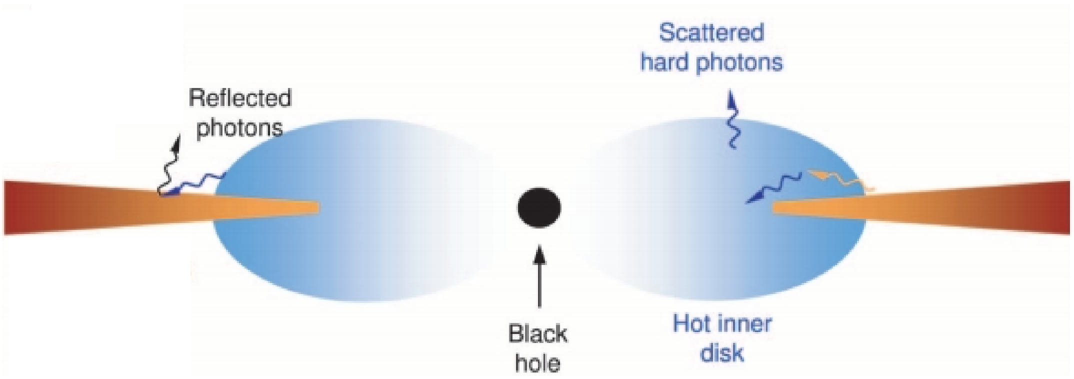

Zdziarski et al. 2002

Dziełak et al. 2019

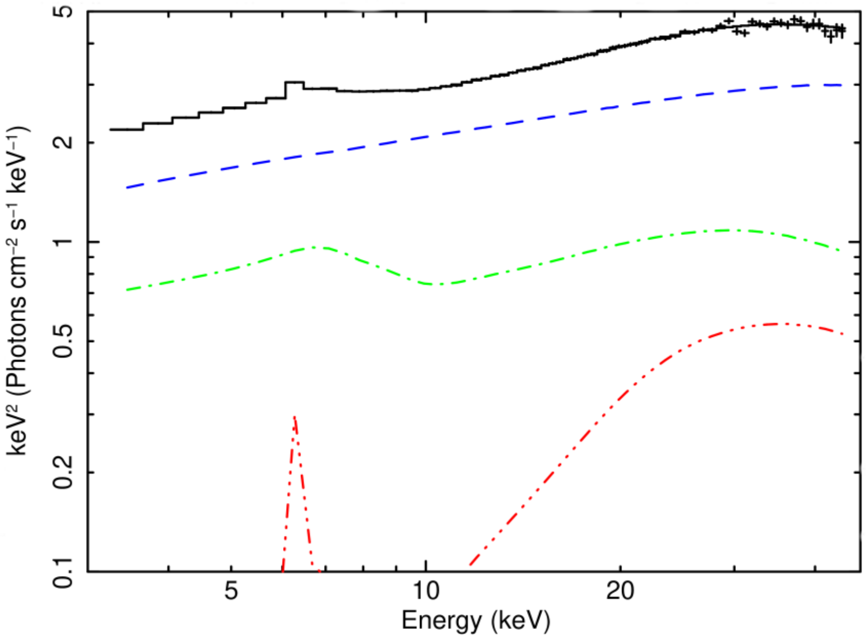

Fitted models

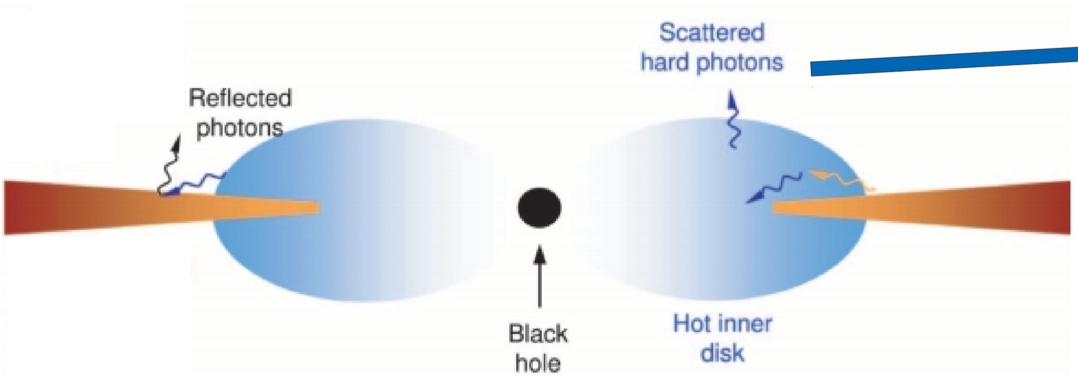

Zdziarski et al. 2002

Dziełak et al. 2019

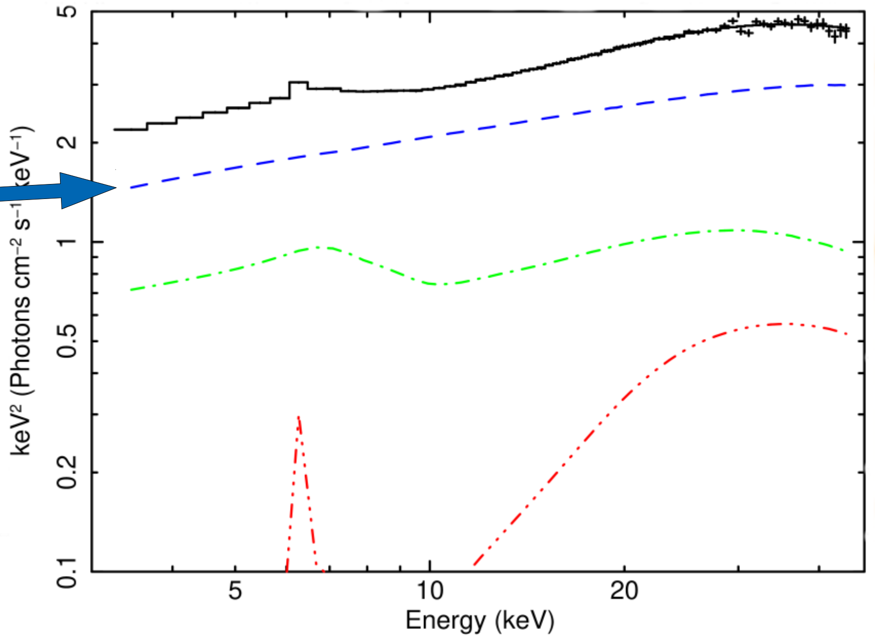

Fitted models

inner, relativistic

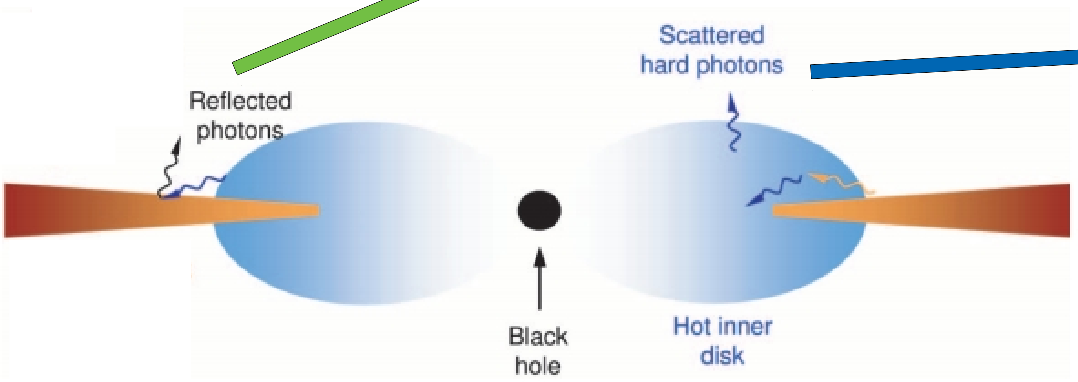

Zdziarski et al. 2002

Dziełak et al. 2019

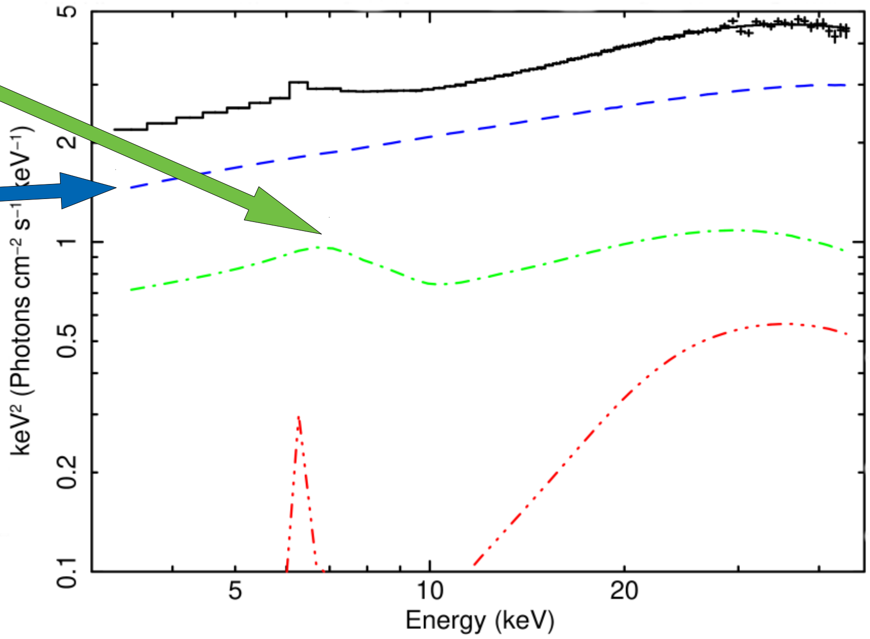

Fitted models

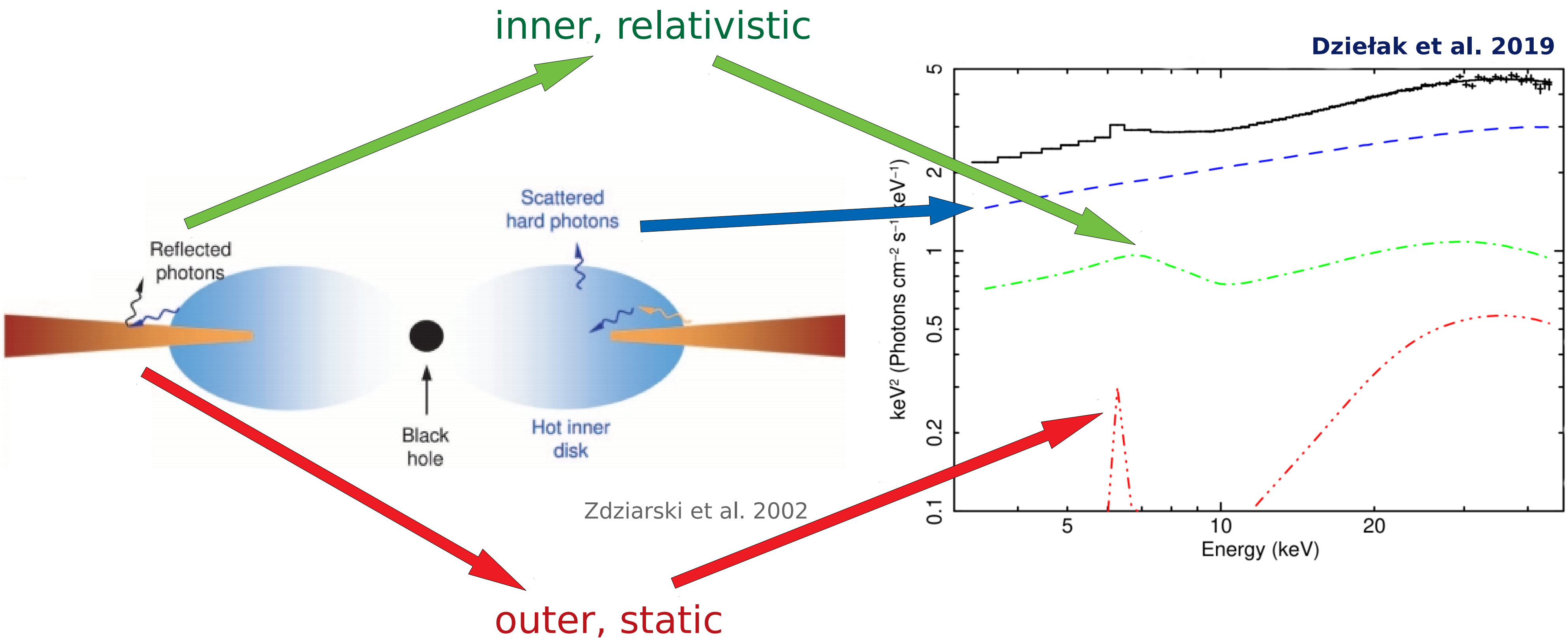

Fitted models

Model: relativistic + static

Model 0: [relxill **(free Z_{Fe})** + xillver **(Z_{Fe} = 1)**]gabs;

relxill

Models 1 and 2: relxill + xillver;

→ two different iron abundances

Model 3: relxillD + xillverD;

reflkerr[1]

Models 4 and 5: reflkerrExp + hreflectExp;

Model 0 follows the original assumptions of Garcia, et al. 2015.

Model 6: reflkerr + hreflect.

1) https://users.camk.edu.pl/mitsza/reflkerr/

Fitted models

Model: relativistic + static

Model 0: [relxill **(free Z_{Fe})** + xillver **(Z_{Fe} = 1)**]gabs;

relxill

Models 1 and 2: relxill + xillver;

→ one iron abundance

Model 3: relxillD + xillverD;

reflkerr[1]

Models 4 and 5: reflkerrExp + hreflectExp;

Model 6: reflkerr + hreflect.

1) https://users.camk.edu.pl/mitsza/reflkerr/

Fitted models

Model: relativistic + static

Model 0: [relxill **(free Z_{Fe})** + xillver **(Z_{Fe} = 1)**]gabs;

relxill

Models 1 and 2: relxill + xillver;

→ one iron abundance

Model 3: relxillD + xillverD;

Data allow for ionization parameters interchange.

reflkerr[1]

Models 4 and 5: reflkerrExp + hreflectExp;

Model 6: reflkerr + hreflect.

1) https://users.camk.edu.pl/mitsza/reflkerr/

Fitted models

Model: relativistic + static

Model 0: [relxill **(free Z_{Fe})** + xillver **(Z_{Fe} = 1)**]gabs;

relxill

Models 1 and 2: relxill + xillver;

→ one iron abundance

→ high density of the disc

Model 3: relxillD + xillverD;

reflkerr[1]

Models 4 and 5: reflkerrExp + hreflectExp;

Model 6: reflkerr + hreflect.

1) https://users.camk.edu.pl/mitsza/reflkerr/

Fitted models

Model: relativistic + static

Model 0: [relxill **(free Z_{Fe})** + xillver **(Z_{Fe} = 1)**]gabs;

relxill

Models 1 and 2: relxill + xillver;

→ one iron abundance

Model 3: relxillD + xillverD;

reflkerr[1]

Models 4 and 5: reflkerrExp + hreflectExp;

Model 6: reflkerr + hreflect.

1) https://users.camk.edu.pl/mitsza/reflkerr/

Fitted models

Model: relativistic + static

Model 0: [relxill **(free Z_{Fe})** + xillver **(Z_{Fe} = 1)**]gabs;

relxill

Models 1 and 2: relxill + xillver;

→ one iron abundance

→ incident e-folded power law

Model 3: relxillD + xillverD;

reflkerr[1]

Models 4 and 5: reflkerrExp + hreflectExp;

Model 6: reflkerr + hreflect.

1) https://users.camk.edu.pl/mitsza/reflkerr/

Fitted models

Model: relativistic + static

Model 0: [relxill **(free Z_{Fe})** + xillver **(Z_{Fe} = 1)**]gabs;

relxill

Models 1 and 2: relxill + xillver;

Model 3: relxillD + xillverD;

reflkerr[1]

Models 4 and 5: reflkerrExp + hreflectExp;

Model 6: reflkerr + hreflect.

→ one iron abundance

→ incident e-folded power law

Data allow for ionization parameters interchange.

1) https://users.camk.edu.pl/mitsza/reflkerr/

Fitted models

Model: relativistic + static

relxill

Model 0: [relxill **(free Z_{Fe})** + xillver **(Z_{Fe} = 1)**]gabs;

Models 1 and 2: relxill + xillver;

→ one iron abundance

Model 3: relxillD + xillverD;

reflkerr[1]

Models 4 and 5: reflkerrExp + hreflectExp;

Model 6: reflkerr + hreflect.

1) https://users.camk.edu.pl/mitsza/reflkerr/

Fitted models

Model: relativistic + static

Model 0: [relxill **(free Z_{Fe})** + xillver **(Z_{Fe} = 1)**]gabs;

relxill

Models 1 and 2: relxill + xillver;

→ one iron abundance

→ incident thermal Comptonization

Model 3: relxillD + xillverD;

reflkerr[1]

Models 4 and 5: reflkerrExp + hreflectExp;

Model 6: reflkerr + hreflect.

1) https://users.camk.edu.pl/mitsza/reflkerr/

Results

	relxill				reflkerr		
Parameter/Model	0	1	2	3	4	5	6
$N_H/10^{21}$ cm^{-2}	$5.2^{+1.8}_{-1.2}$	$4.7^{+1.5}_{-0.3}$	$6.5^{+1.3}_{-1.7}$	$6.1^{+0.7}_{-0.6}$	$4.4^{+1.9}_{-0.4}$	$6.4^{+0.8}_{-1.1}$	$4.3^{+0.5}_{-0.3}$
Γ	$1.70^{+0.07}_{-0.04}$	$1.66^{+0.03}_{-0.04}$	$1.72^{+0.02}_{-0.03}$	$1.70^{+0.01}_{-0.05}$	$1.66^{+0.06}_{-0.02}$	$1.72^{+0.03}_{-0.01}$	–
y	–	–	–	–	–	–	$1.19^{+0.05}_{-0.08}$
E_{cut}	200^{+130}_{-50}	250^{+50}_{-20}	300^{+80}_{-50}	300f	240^{+50}_{-50}	280^{+50}_{-20}	–
$kT_e/1$ keV	–	–	–	–	–	–	20^{+3}_{-2}
R_{in}/R_{ISCO}	11^{+10}_{-10}	19^{+33}_{-6}	$53^{+\infty}_{-26}$	$55^{+\infty}_{-34}$	15^{+31}_{-12}	$58^{+\infty}_{-28}$	$47^{+\infty}_{-45}$
Z_{Fe}	$8.1^{+1.9}_{-5.5}$	$3.1^{+2.0}_{-0.3}$	$2.4^{+0.3}_{-0.2}$	$4.9^{+4.1}_{-0.9}$	$3.9^{+0.8}_{-1.4}$	$2.6^{+0.6}_{-0.4}$	$3.3^{+1.7}_{-1.0}$
$i\,[°]$	29^{+31}_{-29}	3^{+33}_{-3}	43^{+17}_{-23}	3^{+43}_{-3}	9^{+32}_{-9}	43^{+21}_{-19}	49^{+34}_{-26}
$\mathcal{R}$ (inner)	$0.059^{+0.001}_{-0.001}$	$0.170^{+0.004}_{-0.005}$	$0.144^{+0.004}_{-0.003}$	$0.059^{+0.033}_{-0.006}$	$0.25^{+0.04}_{-0.19}$	$0.35^{+0.06}_{-0.12}$	$0.42^{+0.36}_{-0.12}$
$\log_{10}\xi$ (inner)	$3.7^{+0.2}_{-0.5}$	$3.9^{+0.1}_{-0.1}$	$0.0^{+2.3}$	$3.7^{+0.1}_{-0.1}$	$3.9^{+0.1}_{-0.1}$	$1.7^{+0.7}_{-1.7}$	$3.9^{+0.1}_{-0.3}$
$\log_{10}\xi$ (outer)	0f	$1.7^{+0.5}_{-1.7}$	$3.8^{+0.2}_{-0.3}$	$0.7^{+1.0}_{-0.3}$	$2.0^{+0.3}_{-0.4}$	$3.7^{+0.1}_{-0.3}$	0f
$n_e/1$ cm^{-3}	10^{15}f	10^{15}f	10^{15}f	10^{19}f	10^{15}f	10^{15}f	10^{15}f
δ(gabs)	$0.011^{+0.011}_{-0.009}$	–	–	–	–	–	–
$kT_{bb}/1$ keV	–	–	–	–	–	–	$0.34^{+0.04}_{-0.09}$
χ^2_ν	65.6/61	68.7/61	68.3/61	72.4/62	69.1/61	69.2/61	62.1/61
p_i (AIC)	0.136	0.007	0.008	0.018	0.024	0.023	0.784
f_{sc}	$0^{+0.50}$	$0^{+0.15}$	$0^{+0.95}$	$0^{+0.02}$	$0^{+0.13}$	$0^{+0.37}$	$0.20^{+0.27}_{-0.20}$

Our results are significantly model-dependent.

Dziełak et al. 2019

Results

	relxill				reflkerr		
Parameter/Model	0	1	2	3	4	5	6
$N_H / 10^{21}$ cm^{-2}	$5.2^{+1.8}_{-1.2}$	$4.7^{+1.5}_{-0.3}$	$6.5^{+1.3}_{-1.7}$	$6.1^{+0.7}_{-0.6}$	$4.4^{+1.9}_{-0.4}$	$6.4^{+0.8}_{-1.1}$	$4.3^{+0.5}_{-0.3}$
Γ	$1.70^{+0.07}_{-0.04}$	$1.66^{+0.03}_{-0.04}$	$1.72^{+0.02}_{-0.03}$	$1.70^{+0.01}_{-0.05}$	$1.66^{+0.06}_{-0.02}$	$1.72^{+0.03}_{-0.01}$	–
y	–	–	–	–	–	–	$1.19^{+0.05}_{-0.08}$
E_{cut}	200^{+130}_{-50}	250^{+50}_{-20}	300^{+80}_{-50}	300f	240^{+50}_{-50}	280^{+50}_{-20}	–
$kT_e / 1$ keV	–	–	–	–	–	–	20^{+3}_{-2}
R_{in} / R_{ISCO}	11^{+10}_{-10}	19^{+33}_{-6}	$53^{+\infty}_{-26}$	$55^{+\infty}_{-34}$	15^{+31}_{-12}	$58^{+\infty}_{-28}$	$47^{+\infty}_{-45}$
Z_{Fe}	$8.1^{+1.9}_{-5.5}$	$3.1^{+2.0}_{-0.3}$	$2.4^{+0.3}_{-0.2}$	$4.9^{+4.1}_{-0.9}$	$3.9^{+0.8}_{-1.4}$	$2.6^{+0.6}_{-0.4}$	$3.3^{+1.7}_{-1.0}$
$i\,[°]$	29^{+31}_{-29}	3^{+33}_{-3}	43^{+17}_{-23}	3^{+43}_{-3}	9^{+32}_{-9}	43^{+21}_{-19}	49^{+34}_{-26}
$\mathcal{R}$ (inner)	$0.059^{+0.001}_{-0.001}$	$0.170^{+0.004}_{-0.005}$	$0.144^{+0.004}_{-0.003}$	$0.059^{+0.033}_{-0.006}$	$0.25^{+0.04}_{-0.19}$	$0.35^{+0.06}_{-0.12}$	$0.42^{+0.36}_{-0.12}$
$\log_{10} \xi$ (inner)	$3.7^{+0.2}_{-0.5}$	$3.9^{+0.1}_{-0.1}$	$0.0^{+2.3}$	$3.7^{+0.1}_{-0.1}$	$3.9^{+0.1}_{-0.1}$	$1.7^{+0.7}_{-1.7}$	$3.9^{+0.1}_{-0.3}$
$\log_{10} \xi$ (outer)	0f	$1.7^{+0.5}_{-1.7}$	$3.8^{+0.2}_{-0.3}$	$0.7^{+1.0}_{-0.3}$	$2.0^{+0.3}_{-0.4}$	$3.7^{+0.1}_{-0.3}$	0f
$n_e / 1$ cm^{-3}	10^{15}f	10^{15}f	10^{15}f	10^{19}f	10^{15}f	10^{15}f	10^{15}f
δ(gabs)	$0.011^{+0.011}_{-0.009}$	–	–	–	–	–	–
$kT_{bb} / 1$ keV	–	–	–	–	–	–	$0.34^{+0.04}_{-0.09}$
χ^2_ν	65.6/61	68.7/61	68.3/61	72.4/62	69.1/61	69.2/61	62.1/61
p_i (AIC)	0.136	0.007	0.008	0.018	0.024	0.023	0.784
f_{sc}	$0^{+0.50}$	$0^{+0.15}$	$0^{+0.95}$	$0^{+0.02}$	$0^{+0.13}$	$0^{+0.37}$	$0.20^{+0.27}_{-0.20}$

Our results are significantly model-dependent.

Dziełak et al. 2019

Results

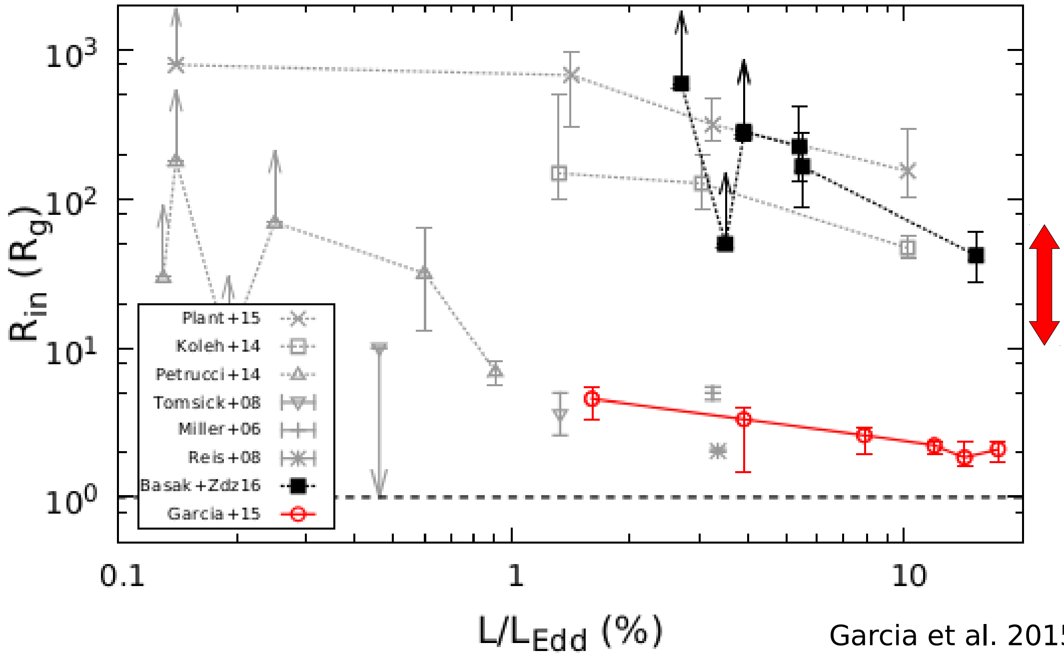

Garcia et al. 2015

All of the models show best-fits consistent with truncation of a disc.

R_{in}/R_{ISCO}	11^{+10}_{-10}	19^{+33}_{-6}	$53^{+\infty}_{-26}$	$55^{+\infty}_{-34}$	15^{+31}_{-12}	$58^{+\infty}_{-28}$	$47^{+\infty}_{-45}$

Dziełak et al. 2019

Results

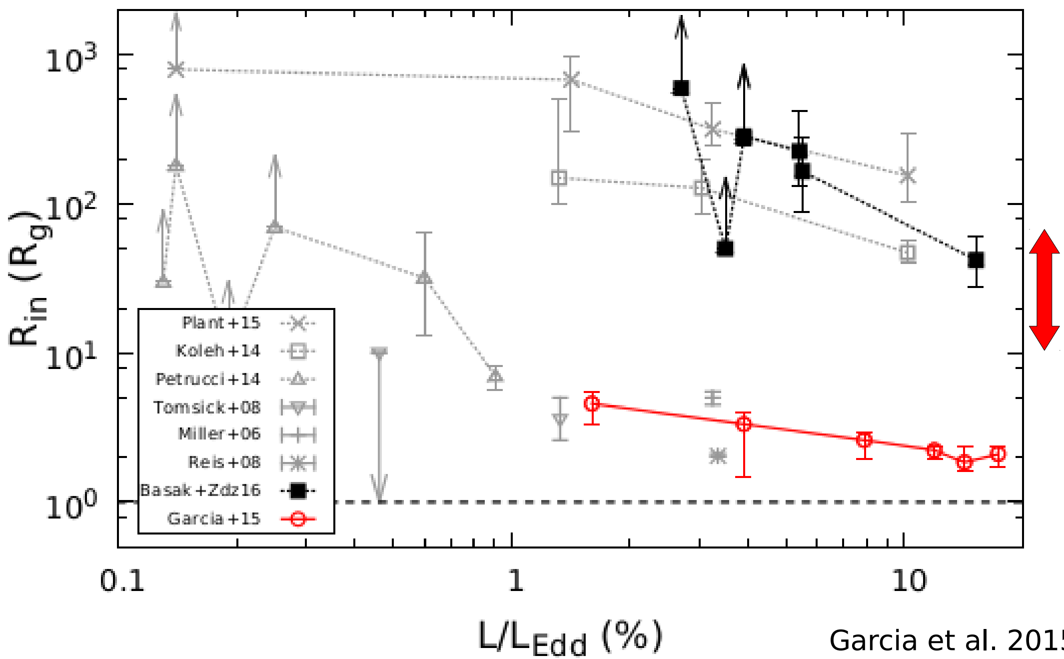

Garcia et al. 2015

All of the models show best-fits consistent with truncation of a disc.

Z_{Fe}	$8.1^{+1.9}_{-5.5}$	$3.1^{+2.0}_{-0.3}$	$2.4^{+0.3}_{-0.2}$	$4.9^{+4.1}_{-0.9}$	$3.9^{+0.8}_{-1.4}$	$2.6^{+0.6}_{-0.4}$	$3.3^{+1.7}_{-1.0}$
R_{in}/R_{ISCO}	11^{+10}_{-10}	19^{+33}_{-6}	$53^{+\infty}_{-26}$	$55^{+\infty}_{-34}$	15^{+31}_{-12}	$58^{+\infty}_{-28}$	$47^{+\infty}_{-45}$

Dziełak et al. 2019

Results

	relxill				reflkerr		
Parameter/Model	0	1	2	3	4	5	6
$N_{\mathrm{H}}/10^{21}\ \mathrm{cm}^{-2}$	$5.2^{+1.8}_{-1.2}$	$4.7^{+1.5}_{-0.3}$	$6.5^{+1.3}_{-1.7}$	$6.1^{+0.7}_{-0.6}$	$4.4^{+1.9}_{-0.4}$	$6.4^{+0.8}_{-1.1}$	$4.3^{+0.5}_{-0.3}$
Γ	$1.70^{+0.07}_{-0.04}$	$1.66^{+0.03}_{-0.04}$	$1.72^{+0.02}_{-0.03}$	$1.70^{+0.01}_{-0.05}$	$1.66^{+0.06}_{-0.02}$	$1.72^{+0.03}_{-0.01}$	–
y	–	–	–	–	–	–	$1.19^{+0.05}_{-0.08}$
E_{cut}	200^{+130}_{-50}	250^{+50}_{-20}	300^{+80}_{-50}	300f	240^{+50}_{-50}	280^{+50}_{-20}	–
$kT_{\mathrm{e}}/1\ \mathrm{keV}$	–	–	–	–	–	–	20^{+3}_{-2}
$R_{\mathrm{in}}/R_{\mathrm{ISCO}}$	11^{+10}_{-10}	19^{+33}_{-6}	$53^{+\infty}_{-26}$	$55^{+\infty}_{-34}$	15^{+31}_{-12}	$58^{+\infty}_{-28}$	$47^{+\infty}_{-45}$
Z_{Fe}	$8.1^{+1.9}_{-5.5}$	$3.1^{+2.0}_{-0.3}$	$2.4^{+0.3}_{-0.2}$	$4.9^{+4.1}_{-0.9}$	$3.9^{+0.8}_{-1.4}$	$2.6^{+0.6}_{-0.4}$	$3.3^{+1.7}_{-1.0}$
$i\,[^\circ]$	29^{+31}_{-29}	3^{+33}_{-3}	43^{+17}_{-23}	3^{+43}_{-3}	9^{+32}_{-9}	43^{+21}_{-19}	49^{+34}_{-26}
$\mathcal{R}$ (inner)	$0.059^{+0.001}_{-0.001}$	$0.170^{+0.004}_{-0.005}$	$0.144^{+0.004}_{-0.003}$	$0.059^{+0.033}_{-0.006}$	$0.25^{+0.04}_{-0.19}$	$0.35^{+0.06}_{-0.12}$	$0.42^{+0.36}_{-0.12}$
$\log_{10}\xi$ (inner)	$3.7^{+0.2}_{-0.5}$	$3.9^{+0.1}_{-0.1}$	$0.0^{+2.3}$	$3.7^{+0.1}_{-0.1}$	$3.9^{+0.1}_{-0.1}$	$1.7^{+0.7}_{-1.7}$	$3.9^{+0.1}_{-0.3}$
$\log_{10}\xi$ (outer)	0f	$1.7^{+0.5}_{-1.7}$	$3.8^{+0.2}_{-0.3}$	$0.7^{+1.0}_{-0.3}$	$2.0^{+0.3}_{-0.4}$	$3.7^{+0.1}_{-0.3}$	0f
$n_{\mathrm{e}}/1\ \mathrm{cm}^{-3}$	10^{15}f	10^{15}f	10^{15}f	10^{19}f	10^{15}f	10^{15}f	10^{15}f
δ(gabs)	$0.011^{+0.011}_{-0.009}$	–	–	–	–	–	–
$kT_{\mathrm{bb}}/1\ \mathrm{keV}$	–	–	–	–	–	–	$0.34^{+0.04}_{-0.09}$
χ^2_ν	65.6/61	68.7/61	68.3/61	72.4/62	69.1/61	69.2/61	62.1/61
p_i (AIC)	0.136	0.007	0.008	0.018	0.024	0.023	0.784
f_{sc}	$0^{+0.50}$	$0^{+0.15}$	$0^{+0.95}$	$0^{+0.02}$	$0^{+0.13}$	$0^{+0.37}$	$0.20^{+0.27}_{-0.20}$

Data allow for ionization parameters interchange.

Dziełak et al. 2019

Results

		relxill			reflkerr		
Parameter/Model	0	1	2	3	4	5	6
$N_{\mathrm{H}}/10^{21}\ \mathrm{cm}^{-2}$	$5.2^{+1.8}_{-1.2}$	$4.7^{+1.5}_{-0.3}$	$6.5^{+1.3}_{-1.7}$	$6.1^{+0.7}_{-0.6}$	$4.4^{+1.9}_{-0.4}$	$6.4^{+0.8}_{-1.1}$	$4.3^{+0.5}_{-0.3}$
Γ	$1.70^{+0.07}_{-0.04}$	$1.66^{+0.03}_{-0.04}$	$1.72^{+0.02}_{-0.03}$	$1.70^{+0.01}_{-0.05}$	$1.66^{+0.06}_{-0.02}$	$1.72^{+0.03}_{-0.01}$	–
y	–	–	–	–	–	–	$1.19^{+0.05}_{-0.08}$
E_{cut}	200^{+130}_{-50}	250^{+50}_{-20}	300^{+80}_{-50}	300f	240^{+50}_{-50}	280^{+50}_{-20}	–
$kT_{\mathrm{e}}/1\ \mathrm{keV}$	–	–	–	–	–	–	20^{+3}_{-2}
$R_{\mathrm{in}}/R_{\mathrm{ISCO}}$	11^{+10}_{-10}	19^{+33}_{-6}	$53^{+\infty}_{-26}$	$55^{+\infty}_{-34}$	15^{+31}_{-12}	$58^{+\infty}_{-28}$	$47^{+\infty}_{-45}$
Z_{Fe}	$8.1^{+1.9}_{-5.5}$	$3.1^{+2.0}_{-0.3}$	$2.4^{+0.3}_{-0.2}$	$4.9^{+4.1}_{-0.9}$	$3.9^{+0.8}_{-1.4}$	$2.6^{+0.6}_{-0.4}$	$3.3^{+1.7}_{-1.0}$
$i\,[^\circ]$	29^{+31}_{-29}	3^{+33}_{-3}	43^{+17}_{-23}	3^{+43}_{-3}	9^{+32}_{-9}	43^{+21}_{-19}	49^{+34}_{-26}
$\mathcal{R}$ (inner)	$0.059^{+0.001}_{-0.001}$	$0.170^{+0.004}_{-0.005}$	$0.144^{+0.004}_{-0.003}$	$0.059^{+0.033}_{-0.006}$	$0.25^{+0.04}_{-0.19}$	$0.35^{+0.06}_{-0.12}$	$0.42^{+0.36}_{-0.12}$
$\log_{10}\xi$ (inner)	$3.7^{+0.2}_{-0.5}$	$3.9^{+0.1}_{-0.1}$	$0.0^{+2.3}$	$3.7^{+0.1}_{-0.1}$	$3.9^{+0.1}_{-0.1}$	$1.7^{+0.7}_{-1.7}$	$3.9^{+0.1}_{-0.3}$
$\log_{10}\xi$ (outer)	0f	$1.7^{+0.5}_{-1.7}$	$3.8^{+0.2}_{-0.3}$	$0.7^{+1.0}_{-0.3}$	$2.0^{+0.3}_{-0.4}$	$3.7^{+0.1}_{-0.3}$	0f
$n_{\mathrm{e}}/1\ \mathrm{cm}^{-3}$	10^{15}f	10^{15}f	10^{15}f	10^{19}f	10^{15}f	10^{15}f	10^{15}f
δ(gabs)	$0.011^{+0.011}_{-0.009}$	–	–	–	–	–	–
$kT_{\mathrm{bb}}/1\ \mathrm{keV}$	–	–	–	–	–	–	$0.34^{+0.04}_{-0.09}$
χ^2_ν	65.6/61	68.7/61	68.3/61	72.4/62	69.1/61	69.2/61	62.1/61
p_i (AIC)	0.136	0.007	0.008	0.018	0.024	0.023	0.784
f_{sc}	$0^{+0.50}$	$0^{+0.15}$	$0^{+0.95}$	$0^{+0.02}$	$0^{+0.13}$	$0^{+0.37}$	$0.20^{+0.27}_{-0.20}$

Data allow for ionization parameters interchange.

- the relatively modest relativistic effects

Dziełak et al. 2019

Results

reflkerr

Parameter/Model	0	1	2	3	4	5	6
$N_{\mathrm{H}}/10^{21}\,\mathrm{cm}^{-2}$	$5.2^{+1.8}_{-1.2}$	$4.7^{+1.5}_{-0.3}$	$6.5^{+1.3}_{-1.7}$	$6.1^{+0.7}_{-0.6}$	$4.4^{+1.9}_{-0.4}$	$6.4^{+0.8}_{-1.1}$	$4.3^{+0.5}_{-0.3}$
Γ	$1.70^{+0.07}_{-0.04}$	$1.66^{+0.03}_{-0.04}$	$1.72^{+0.02}_{-0.03}$	$1.70^{+0.01}_{-0.05}$	$1.66^{+0.06}_{-0.02}$	$1.72^{+0.03}_{-0.01}$	–
y	–	–	–	–	–	–	$1.19^{+0.05}_{-0.08}$
E_{cut}	200^{+130}_{-50}	250^{+50}_{-20}	300^{+80}_{-50}	300f	240^{+50}_{-50}	280^{+50}_{-20}	–
$kT_{\mathrm{e}}/1\,\mathrm{keV}$	–	–	–	–	–	–	20^{+3}_{-2}
$R_{\mathrm{in}}/R_{\mathrm{ISCO}}$	11^{+10}_{-10}	19^{+33}_{-6}	$53^{+\infty}_{-26}$	$55^{+\infty}_{-34}$	15^{+31}_{-12}	$58^{+\infty}_{-28}$	$47^{+\infty}_{-45}$
Z_{Fe}							$3.3^{+1.7}_{-1.0}$
$i\,[^\circ]$							49^{+34}_{-26}
$\mathcal{R}$ (inner)							$0.42^{+0.36}_{-0.12}$
$\log_{10}\xi$ (inner)							$3.9^{+0.1}_{-0.3}$
$\log_{10}\xi$ (outer)							0f
$n_{\mathrm{e}}/1\,\mathrm{cm}^{-3}$							10^{15}f
δ(gabs)							–
$kT_{\mathrm{bb}}/1\,\mathrm{keV}$							$0.34^{+0.04}_{-0.09}$
χ^2_ν							62.1/61
p_i (AIC)							0.784
f_{sc}							$0.20^{+0.27}_{-0.20}$

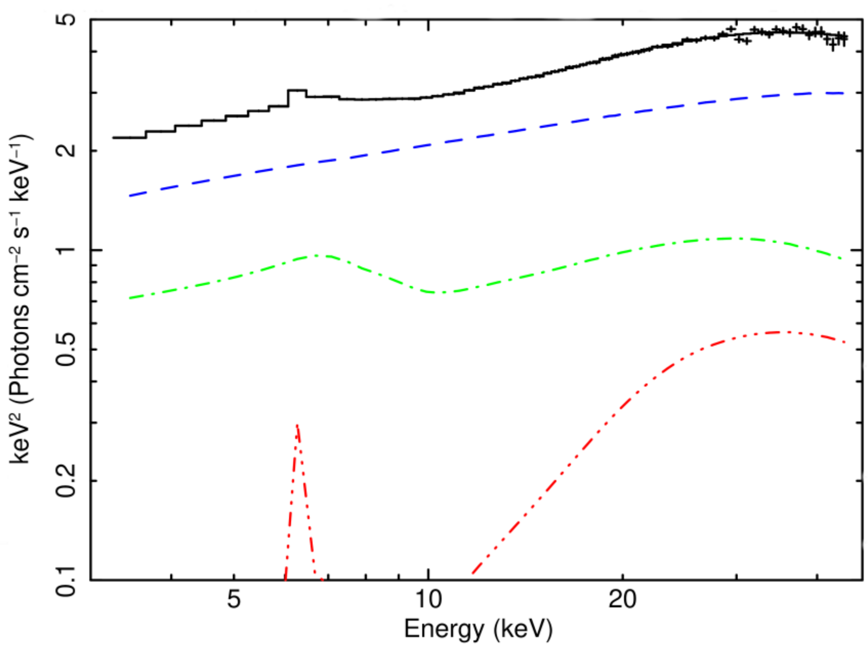

Thermal Comptonization (blue) and two reflectors, an inner one (green) and an outer one (red). The solid shows the total model.

Dziełak et al. 2019

Our statistically best model has a physical *thermal-Comptonization* primary continuum.

The best fit value of the truncation radius

is **47 R_{ISCO}**,

and **R_{in} >~ 2R_{ISCO}**

(90% confidence limits)

Results

Comptonization of the reflected component (Steiner et al. 2017)

- this effect is minor

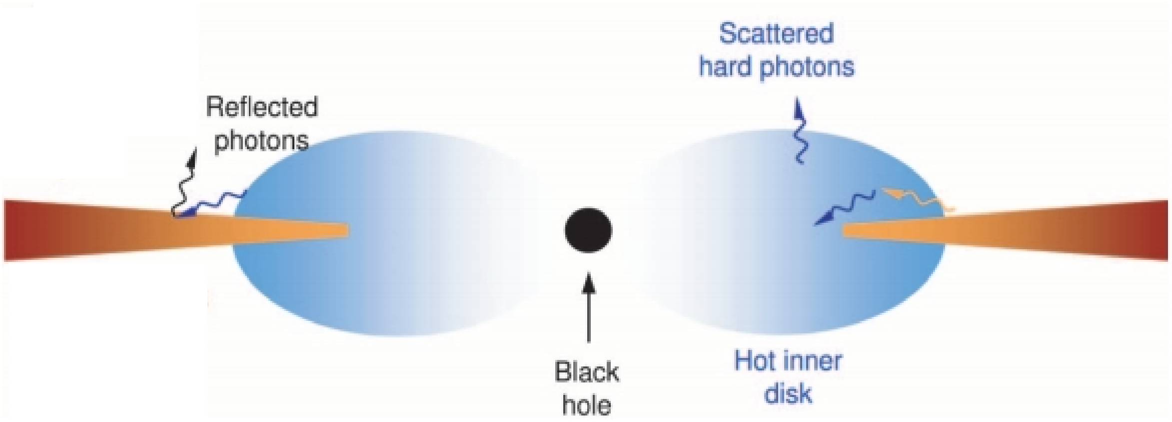

Zdziarski et al. 2002

Results

Reflector density

The model of Garcıa et al. (2016) with $\mathbf{n_e = 10^{19}\,cm^{-3}}$

- **increase of both the truncation radius** and **the Fe abundance**

- at odd with Tomsick et al. (2018)

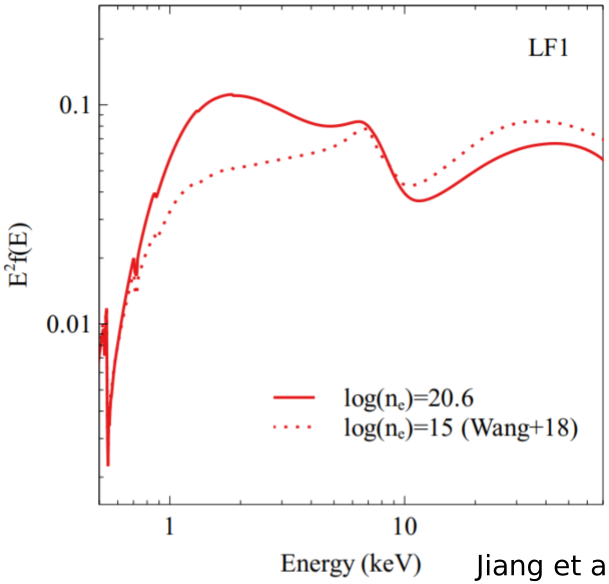

Jiang et al. 2019

Conclusions

Analysed spectra can be fitted with similar quality with models allowing significantly different disc truncation radii.

Still, all of the fitted models prefer the R_{in} much larger than R_{ISCO} at their best-fit values.

Breaking degeneracy

→ Use **spectral-timing analysis** to break degeneracy of spectral fitting alone.

→ Use additional information from fast variability of the source.

→ Reconstruct **the energy spectra of the different variability components**.

Breaking degeneracy

→ Use **spectral-timing analysis** to break degeneracy of spectral fitting alone.

→ Use additional information from fast variability of the source.

→ Reconstruct **the energy spectra of the different variability components**.

→ To study **stratification of accretion flow** and **distinguish between different models** (Axelsson & Done 2018, Mahmoud et al. 2019).

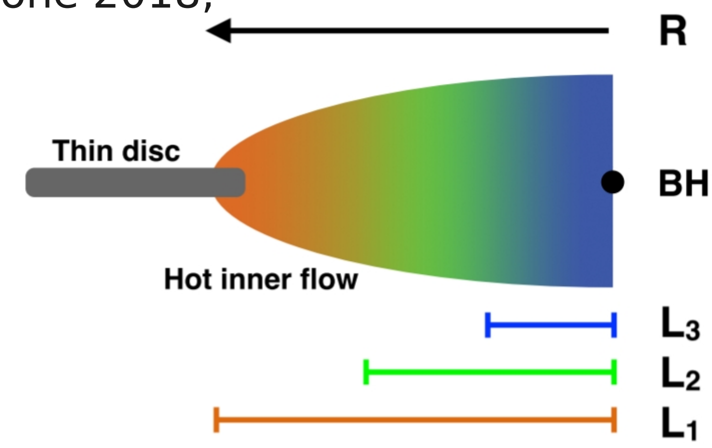

Conclusions

Analysed spectra can be fitted with similar quality with models allowing significantly different disc truncation radii.

Still, all of the fitted models prefer the R_{in} much larger than R_{ISCO} at their best-fit values.

Use **spectral-timing analysis** to break degeneracy of spectral fitting alone.

Satelites

Plant+15 – XMM and Suzaku

Kolehmainen+14 – XMM and RXTE

Petrucci+14 – Suzaku

Tomsick+08 – Swift and RXTE

Miller+06 – XMM and RXTE

Reis+08 – XMM and RXTE

Basak+Zdziarski16 - XMM

Garcia+15 – RXTE

Dziełak+19 – RXTE

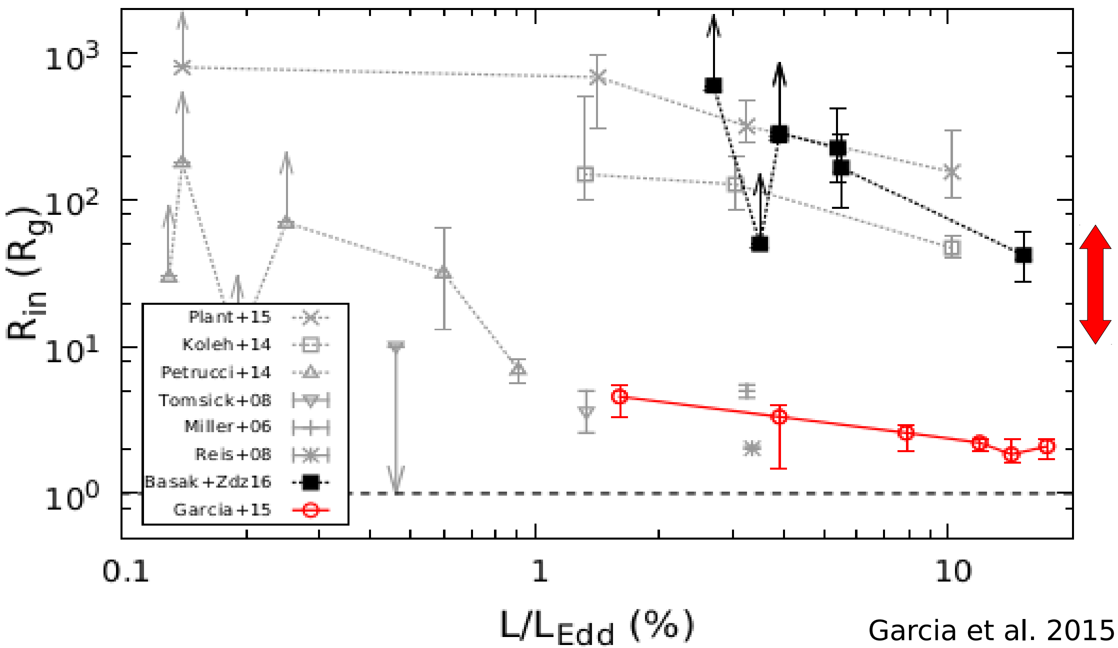

Garcia et al. 2015